

2013

Synthesis and characterization of vegetable oil-based polyurethane dispersions

Thomas Frederick Garrison
Iowa State University

Follow this and additional works at: <https://lib.dr.iastate.edu/etd>

 Part of the [Polymer Chemistry Commons](#)

Recommended Citation

Garrison, Thomas Frederick, "Synthesis and characterization of vegetable oil-based polyurethane dispersions" (2013). *Graduate Theses and Dissertations*. 13470.
<https://lib.dr.iastate.edu/etd/13470>

This Dissertation is brought to you for free and open access by the Iowa State University Capstones, Theses and Dissertations at Iowa State University Digital Repository. It has been accepted for inclusion in Graduate Theses and Dissertations by an authorized administrator of Iowa State University Digital Repository. For more information, please contact digirep@iastate.edu.

Synthesis and characterization of vegetable oil-based polyurethane dispersions

by

Thomas F. Garrison

A dissertation submitted to the graduate faculty
in partial fulfillment of the requirements for the degree of

DOCTOR OF PHILOSOPHY

Major: Chemistry

Program of Study Committee:

Richard C. Larock, Co-major Professor

Michael R. Kessler, Co-major Professor

Malika Jeffries-EL

Arthur Winter

Keith Woo

Iowa State University

Ames, Iowa

2013

Copyright © Thomas F. Garrison, 2013. All rights reserved.

DEDICATION

To Andrea
for all your sacrifices and support

TABLE OF CONTENTS

DEDICATION	ii
LIST OF ABBREVIATIONS	v
CHAPTER 1. GENERAL INTRODUCTION	1
Overview	1
Background	2
References	7
CHAPTER 2. EFFECT OF UNSATURATION ON VEGETABLE OIL-BASED POLYURETHANE COATINGS	9
Abstract	9
Introduction	10
Experimental	17
Results and Discussion	21
Conclusions	30
Acknowledgements	31
References	31
CHAPTER 3. MECHANICAL AND ANTIBACTERIAL PROPERTIES OF SOYBEAN- OIL-BASED CATIONIC POLYURETHANE COATINGS: EFFECTS OF AMINE RATIO AND DEGREE OF CROSSLINKING	34
Abstract	34
Introduction	35
Experimental	37
Results and Discussion	44
Conclusions	55
Acknowledgments	56
References	56
CHAPTER 4. EFFECTS OF COUNTERIONS ON THE PHYSICAL AND ANTIMICROBIAL PROPERTIES OF CASTOR OIL-BASED CATIONIC POLYURETHANE COATINGS	58
Introduction	58
Experimental	61
Results and Discussion	63

Conclusions	71
Acknowledgements	72
References	72
CHAPTER 5. GRAFTED HYBRID LATEXES FROM CASTOR OIL-BASED WATERBORNE POLYURETHANES	74
Abstract	74
Introduction	74
Experimental	78
Results and Discussion	82
Conclusions	90
Acknowledgements	90
References	91
CHAPTER 6. GENERAL CONCLUSIONS	93
ACKNOWLEDGEMENTS	96

LIST OF ABBREVIATIONS

AcO	acetoxy group
AcOH	acetic acid
BA	butyl acrylate
BuOH	butanol
C1 and C2	experimentally determined parameters
DBTDL	dibutyltin dilaurate
DHB	2,5-dihydroxybenzoic acid
DMA	dynamic mechanical analysis
DSC	differential scanning calorimetry
<i>E</i>	Young's modulus
<i>E'</i>	storage modulus
ESO	epoxidized soybean oil
GHL	grafted hybrid latex
HDI	hexamethylene diisocyanate
HEA	2-hydroxyethyl acrylate
IPDI	isophorone diisocyanate
KOH	potassium hydroxide
KPS	potassium persulfate
MALDI-TOF	Matrix-assisted laser desorption/ionization time-of-flight mass spectrometry
MDEA	<i>N</i> -methyl diethanolamine
MEK	methyl ethyl ketone
MeOH	methanol
M_c	molecular weight between crosslinks
M_n	number average molecular weight
M_w	mass average molecular weight
MRSA	methicillin-resistant <i>Staphylococcus aureus</i>
NCO group	isocyanate group

NMR	nuclear magnetic resonance
OH	hydroxyl
OH #	hydroxyl number
OM	outer membrane
Pa	Pascal
PDI	polydispersity index
PU	polyurethane
PUD	polyurethane dispersion
R	gas constant
SEC	size exclusion chromatography
ST	styrene
T	absolute temperature
T_g	glass transition temperature
T_5	temperature at 5% weight loss
T_{50}	temperature at 50% weight loss
T_{max}	temperature at maximum degradation
$\tan \delta$	tan delta
TEA	triethylamine
TEM	transmission electron microscope
TGA	thermogravimetric analysis
TG-MS	thermogravimetric analysis – mass spectrometry
TSB	tryptic soy broth
VOC	volatile organic compound
wt%	weight percent
ZOI	zone of inhibition
ε	elongation
ε_b	elongation at break
σ	tensile strength
σ_b	tensile strength at break
λ	stretch ratio
ρ	density

CHAPTER 1. GENERAL INTRODUCTION

Overview

In this thesis, we explore the thermal, mechanical, and antimicrobial properties of bio-based waterborne polyurethane coatings and grafted hybrid latexes made from polyurethane dispersions. Chapter 1 describes the effect of residual unsaturation in epoxidized vegetable oils on the physical and thermal properties of films prepared from anionic polyurethane dispersions. We were able to isolate the effect of residual unsaturation by controlling the extent of epoxidation of the vegetable oils. Matrix-assisted laser desorption/ionization time-of-flight mass spectrometry (MALDI-TOF) was used to accurately determine the molecular weight and mass distribution of the vegetable oil polyols. We also examined the effect of different side groups introduced by ring opening of epoxidized soybean oil. This work will be submitted to *Macromolecular Bioscience*.

Chapters 3 and 4 examine the physical, thermal, and antimicrobial properties of cationic waterborne polyurethane dispersions. This work was conducted in collaboration with microbiologists at Iowa State University. Our collaborators, Dr. Byron Brehm-Stecher and his research group, investigated the modes of action for antimicrobial activity. Previous work by our groups examined the effect of different amine polyols on the thermal, mechanical, and antimicrobial properties of polyurethane films.¹ In Chapter 3, we have examined the effects of adjusting the molar ratio of the *N*-methyl diethanolamine on the physical and antimicrobial properties of the polyurethane films. This work has been submitted to *Biomacromolecules*. Chapter 4 explores the effect of the different counteranions on the physical and antimicrobial properties of the polyurethane films. Evolved gas analysis was used to quantify the residual amounts of acid trapped in the film.

Preliminary antimicrobial testing has been conducted. This work will be submitted for publication after completion of more detailed antimicrobial studies.

Chapter 5 examines the use of 2-hydroxyethyl acrylate (HEA) for introducing graft sites when making grafted hybrid latexes from castor oil-based waterborne dispersions. Previous efforts by our group explored using residual unsaturation in soy polyols and acrylated epoxidized soybean oil as graft sites.^{2,3} In this work, we have estimated the molecular weight between crosslinks using Mooney-Rivlin plots. This work will be submitted to *Macromolecular Materials and Communications*.

Background

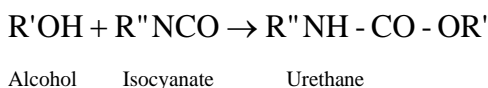
As a precursor to discussion about the advantages and challenges of synthesizing waterborne coatings, it is important to first note some of the characteristics of the conventional organic solvent-based coatings that they replace. Organic solvents are useful because they are effective at dissolving binders and homogenizing coating blends, controlling viscosity, increasing shelf life, and wetting the substrate surface.^{4,5} However, organic solvents pose significant risks due to environmental, industrial, and fire safety concerns.⁵ With greater public and regulatory emphasis on using environmentally-friendly processes, waterborne coatings offer inherent advantages to both consumers and manufacturers.⁶ Processing and manufacturing of coatings account for the second leading source of human caused atmospheric pollutants, behind vehicular traffic.⁴

A key benefit of all waterborne coatings is the reduction in hazardous emissions from volatile organic compounds (VOCs) generated by non-aqueous solvents. Other coating strategies have also been designed to reduce VOCs, including high solids coatings, powder

coatings, and radiation curable coatings.⁷ These other coating systems have their own unique advantages and disadvantages, but are outside the scope of this dissertation.

Polyurethanes. In recent years, considerable research has focused on the replacement of petroleum-based starting materials for polyurethanes with biorenewable-based materials.⁸⁻¹⁰ While the vast majority of research in bio-based polyurethanes has focused on using vegetable oil-based polyols, the development of aliphatic vegetable oil-based isocyanates has also been investigated.¹¹

Polyurethanes are prepared by treating polyols with a slight excess of diisocyanates.¹² In polyurethane dispersions, linear chains with high molecular weights are desired. These linear chains can be obtained by treating low functional polyols (*i.e.* diols) with diisocyanates to form urethanes. The following reaction is called the urethane reaction:



Aqueous polyurethane dispersions are a particularly important class of waterborne coatings. Applications of polyurethane dispersions include floor coatings,¹³ textile coatings,^{14,15} and adhesives.¹⁶ The advantages of polyurethane dispersions are very similar to those of emulsion coatings. The viscosity of polyurethane dispersions is nearly independent of the molecular weight of the polymer.¹⁷ This allows for dispersions with high solid content loadings of high molecular weight polymers to be prepared that yield good coatings by physical drying processes.¹⁷ In comparison to other waterborne coatings, aqueous polyurethane dispersions have the lowest amounts of organic solvent emissions (3 wt%). These low organic solvent emissions approach the low levels typical of powder coatings (0.1 to 4 wt%).⁴

Directly synthesizing polyurethane dispersions in water is not possible because of the reactivity of diisocyanates with water.¹⁸ Several methods for making aqueous polyurethane dispersions have been developed, including the acetone process, the prepolymer mixing process, the melt dispersion process, and the ketimine/ketazine process.¹⁹ The acetone process is one of the most widely used in industry.¹⁹ In the first step, polyurethane chains are extended with hydrophilic groups incorporated into the polymer backbone.¹² The solvent, acetone, reduces the viscosity during the polyurethane synthesis. Water is then added to the mixture to form the dispersion. After dispersion, the acetone can be removed using distillation.²⁰ The acetone process is often modified to use other solvents, such as methyl ethyl ketone, in place of acetone.^{14,21}

Emulsion Coatings. As a precursor to the discussion of hybrid grafted latexes in chapter 4, an introduction to emulsion polymerization and latex coatings is useful. Emulsion polymerization produces latex particles, which are dispersions of fine polymer particles in water.^{7,22,23} Frequently, the terms emulsion coating and latex paint are used interchangeably. Applications of emulsion coatings include paints, coatings, adhesives, and paper coatings.²³

Emulsion coatings have a number of desirable physical properties. Styrene-butadiene latex paints for interior walls were first sold commercially in the United States in the late 1940s.^{24,25} These paints appealed to consumers because of their easy application, low odor, and easy clean-up.^{24,25} Acrylic latexes are known for high molecular weights with good corrosion resistance and are generally more economical than polyurethane coatings.^{5,22,26} However, acrylic latexes have poor film forming properties, abrasion resistance and toughness compared to polyurethane dispersions.^{13,27}

A typical formulation for emulsion polymerization consists of a slightly water-soluble monomer, co-monomers, a water-soluble initiator, surfactants, and any other additives, which are combined in an aqueous solution.⁵ In emulsion polymerization, monomers are polymerized through a free-radical process. The monomer molecules migrate from the monomer droplets to inside surfactant micelles, where the polymerization actually occurs.^{4,5,22} Polymerization begins when a water-soluble initiator molecule enters a micelle and reacts with the monomer. These micelles form when the surfactant concentration is above a minimum concentration, called the critical micelle concentration.²² As polymerization progresses, the monomer droplet size decreases and the size of the polymer-containing micelles increase.^{5,22} The resulting aqueous suspension of polymers is called a latex.²² Figure 1 illustrates the emulsion polymerization process.

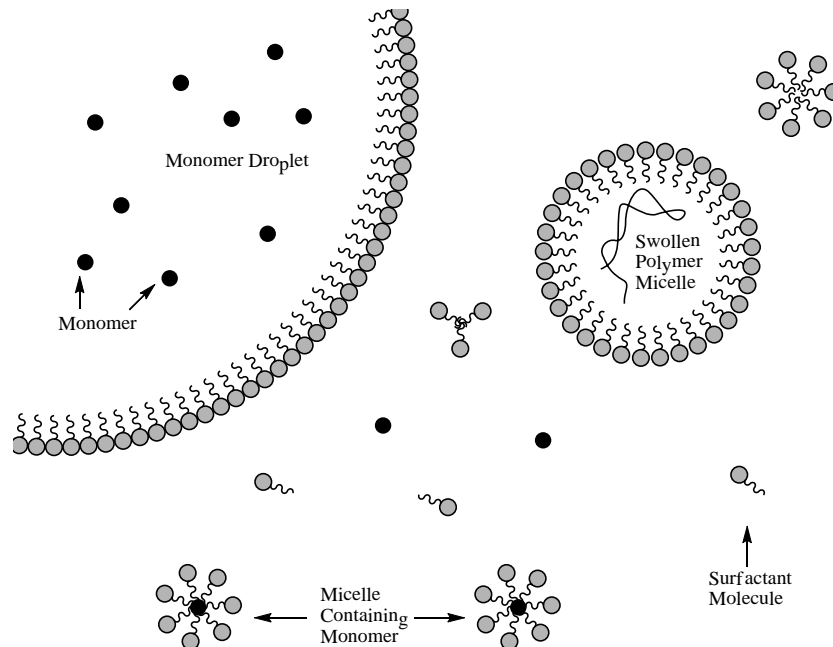


Figure 1. Schematic drawing of emulsion polymerization

Terminology. Frequently, the terminology associated with waterborne coatings is ambiguous and often misused. Products of emulsion polymerization are latexes, a dispersion of polymerized polymer particles. Emulsions are dispersions of liquid droplets in another liquid, such as water.⁷ However, coatings prepared from emulsion polymerization are still commonly referred to as emulsion coatings, which highlight the ambiguity of coating terminology. Given below are definitions of coating terminology:

- *Colloid or colloidal dispersion* – a substance or material consisting of ultra-microscopic particles (solid, liquid, or gas) that has negligible settling when dispersed in a different medium (solid, liquid, or gas).^{24,25,28}
- *Dispersion* – a generic term for a heterogeneous system where a solid, gas, or liquid is dispersed in a different medium.^{24,25,29}
- *Emulsion* – a generic term for a liquid system consisting of fine (but larger than colloidal size) globules of liquid dispersed within a different, immiscible liquid (usually water). Emulsions can be dispersed with or without the use of emulsifiers.^{24,25,29}
- *Latex* – a dispersion or suspension of fine polymer particles in water that resists settling.²²

Particle size is a common way to classify different types of waterborne coatings.^{4,24,25}

Table 1 below lists typical particle sizes of different waterborne coatings. Another approach for classifying coating systems is based on how coating resins are polymerized. Primary dispersions are directly polymerized in water by emulsion polymerization.^{4,25} Secondary

dispersions are polymers dispersed in water after completion of a bulk polymerization process.^{4,25} In the case of colloids, the binders typically have neutralizable groups (usually acidic groups) which are converted to salts. Hydrophilic groups, such as polyglycols, can also be incorporated into the polymer molecule to improve water solubility.⁴

Table 1. Particle size of different waterborne coating systems

Term	Particle size
Solution	below 0.001 μm
Colloid	0.001 to 0.1 μm
Dispersion	above 0.1 μm

References

1. Y. Xia, Z. Zhang, M. R. Kessler, B. Brehm-Stecher and R. C. Larock, *ChemSusChem*, 2012, **5**, 2221.
2. Y. Lu and R. C. Larock, *Biomacromolecules*, 2007, **8**, 3108.
3. Y. Lu and R. C. Larock, *J. Appl. Polym. Sci.*, 2011, **119**, 3305.
4. K. Dören, W. Freitag and D. Stoye, *Water-Borne Coatings: The Environmentally-friendly Alternative*, Hanser Publishers, Munich, 1994.
5. A. Marrion, ed., *The Chemistry and Physics of Coatings*, Royal Society of Chemistry, Cambridge, UK, 1994.
6. K.-L. Noble, *Prog. Org. Coat.*, 1997, **32**, 131.
7. K. D. Weiss, *Prog. Polym. Sci.*, 1997, **22**, 203.
8. M. A. R. Meier, J. O. Metzger and U. S. Schubert, *Chem. Soc. Rev.*, 2007, **36**, 1788.
9. Z. S. Petrovic, *Polym. Rev.*, 2008, **48**, 109.
10. Y. Xia and R. C. Larock, *Green Chem.*, 2010, **12**, 1893.
11. D. P. Pfister, Y. Xia and R. C. Larock, *ChemSusChem*, 2011, **4**, 703.
12. G. N. Manvi and R. N. Jagtap, *J. Disper. Sci. Technol.*, 2010, **31**, 1376.
13. G. A. Howarth, *Surf. Coat. Int. Pt. B-Coat. Trans.*, 2003, **86**, 111.
14. H. Pan and D. Chen, *Text. Res. J.*, 2009, **79**, 687.
15. Q. B. Meng, S.-I. Lee, C. Nah and Y.-S. Lee, *Prog. Org. Coat.*, 2009, **66**, 382.
16. E. Orgilés-Calpena, F. Arán-Aís, A. M. Torró-Palau, C. Orgilés-Barceló and J. M. Martín-Martínez, *Int. J. Adhes. Adhes.*, 2009, **29**, 774.
17. B. K. Kim, *Colloid Polym. Sci.*, 1996, **274**, 599.

18. O. Jaudouin, J. J. Robin, J. M. Lopez-Cuesta, D. Perrin and C. Imbert, *Polym. Int.*, 2012, **61**, 495.
19. V. D. Athawale and R. V. Nimbalkar, *J. Am. Oil Chem. Soc.*, 2011, **88**, 159.
20. H. Sardon, L. Irusta, M. J. Fernandez-Berridi, J. Luna, M. Lansalot and E. Bourgeat-Lami, *J. Appl. Polym. Sci.*, 2011, **120**, 2054.
21. Y. Lu and R. C. Larock, *Biomacromolecules*, 2008, **9**, 3332.
22. J. R. Fried, *Polymer Science & Technology*, Prentice Hall Professional Technical Reference, Upper Saddle River, NJ, 2003.
23. A. M. van Herk, in *Hybrid Latex Particles*, eds. A. M. VanHerk and K. Landfester, Springer-Verlag Berlin, Berlin, 2010, vol. 233, pp. 1-18.
24. C. R. Martens, *Emulsion and Water-Soluble Paints and Coatings*, Reinhold Publishing Corp., New York, 1964.
25. C. R. Martens, *Waterborne Coatings: Emulsion and Water-Soluble Paints*, Van Nostrand Reinhold Co., New York, 1981.
26. A. C. Aznar, O. R. Pardini and J. I. Amalvy, *Prog. Org. Coat.*, 2006, **55**, 43.
27. M. Li, E. S. Daniels, V. Dimonie, E. D. Sudol and M. S. El-Aasser, *Macromolecules*, 2005, **38**, 4183.
28. K. W. Whitten, R. E. Davis and M. L. Peck, *General Chemistry*, Saunders College Publishing, Orlando, FL, 1996.
29. F. C. Mish, ed., *Merriam-Webster's Collegiate Dictionary*, Merriam-Webster Inc., Springfield, MA, 1993.

CHAPTER 2. EFFECT OF UNSATURATION ON VEGETABLE OIL-BASED POLYURETHANE COATINGS

A paper to be submitted to *Macromolecular Bioscience*

Thomas F. Garrison,^a Michael R. Kessler,^{*b-d} and Richard C. Larock^{*a}

^a Department of Chemistry, Iowa State University, Ames, Iowa

^b Department of Materials Science and Engineering, Iowa State University, Ames, Iowa

^c Ames Laboratory, US Dept. of Energy, Ames, Iowa.

^d School of Mechanical and Materials Engineering, Washington State University, Pullman, Washington.

Abstract

A variety of vegetable oil-based, waterborne polyurethane dispersions have been successfully synthesized from different vegetable oil polyols exhibiting almost constant hydroxyl functionalities of 2.7 OH groups per molecule. The vegetable oil polyols, which have been prepared from vegetable oils with different fatty acid compositions (peanut, corn, soybean, and linseed oil), range in residual degree of unsaturation from 0.4 to 3.5 carbon-carbon double bonds per triglyceride molecule. The effects of residual unsaturation on the thermal and mechanical properties of the resulting polyurethane films have been investigated by dynamic mechanical analysis, differential scanning calorimetry, and thermal gravimetric analysis. Matrix-assisted laser desorption/ionization time-of-flight mass spectrometry (MALDI-TOF) has been used to accurately determine the molecular weight and mass distribution of the vegetable oil polyols. Higher residual unsaturation results in polyurethane films with increased break strength, Young's modulus, and toughness. This work has isolated the effect of unsaturation on vegetable oil-based polyurethane films, which has been neglected in previous studies. The effect of different oxirane ring opening methods

(methanol, butanol, acetic acid, and hydrochloric acid) on the properties of the coatings has also been examined.

Introduction

Polyurethanes are versatile materials with applications ranging from production of rigid plastics to soft foams, films, elastomers, and others.¹ Protective and decorative coatings are particularly important applications. In 2012, the total revenue from paints and coatings manufactured in the United States was \$24 billion.² While this amount includes all types of coating materials, polyurethanes account for a substantial portion of this market, particularly in high-end applications.³

Currently, solvent-borne polyurethane raw materials account for 18% of the total value of global consumption of coating materials.³ The Clean Air Act of 1970, as well as more recent legislation in European countries, greatly affected the entire paints and coatings industry by mandating the reduction and monitoring of the release of volatile organic compounds (VOCs) into the atmosphere.⁴ In response to these regulations, manufacturers have sought ways to eliminate organic solvents from paints and coatings. In particular, the focus turned to waterborne polyurethane coatings as an effective means for the reduction of VOC emissions.⁵ By switching to waterborne coatings, manufacturers are realizing additional benefits by reducing material costs associated with organic solvents and reducing fire and health risks.⁶ As a result, waterborne coatings are gaining market share, especially in the European sector.⁷

Currently, coating materials are primarily prepared from petroleum-based materials, linking the supply chain and cost of raw materials to crude oil prices.² Serious, long-term supply issues and environmental risks are major concerns as dwindling conventional

petroleum reserves lead to the increased exploitation of more expensive and environmentally damaging, unconventional oil resources, such as oil sands or oil shale.^{8,9} Economic, political, geological, and environmental concerns may also limit the development of untapped petroleum reserves, especially those located in the Arctic regions.^{10,11} Despite the increase in gas and oil production in the United States, the connection of domestic gas and oil prices to global markets is expected to intensify, creating greater exposure to global price fluctuations.¹⁰ Consequently, manufacturers will be inclined to develop biobased plastics to hedge against the uncertainty of crude oil price fluctuations and other factors limiting future supplies, such as growing oil consumption in Asian and other emerging markets.¹²

Polyurethanes are prepared from two types of reagents: polyols and diisocyanates. More recently, polyurethane coatings made in part from biorenewable sources have been investigated as replacements for petroleum-based feedstocks.¹³⁻¹⁵ Currently, only polyols can be effectively made from biorenewable materials, such as vegetable oils that can be chemically modified to form polyols and replace petroleum-derived polyether and polyester polyols.¹⁵ In addition to vegetable oils, other biorenewable triglycerides, such as fish oil, have also been used to make polyurethane coatings.¹⁶

The purpose of the present research was to examine the effects of carbon-carbon double bonds in the polyol segment on the physical properties of vegetable oil-based polyurethane dispersions. Our investigation focused on whether residual unsaturation is an important variable in the experimental design of such coatings. Previous research has examined the effect of different hydroxyl numbers using soybean oil-based polyols. However, the hydroxyl value and residual carbon-carbon double bond content changed

simultaneously.¹⁷ Other studies have used different vegetable oils and that has been treated such that few or no residual carbon-carbon double bonds remain in the resulting materials.¹⁸

In order to isolate the effects of the extent of unsaturation, several different vegetable oils (peanut oil, corn oil, soybean oil, and linseed oil) were partially epoxidized and subsequently ring-opened to yield vegetable oil polyols with a constant hydroxyl functionality. Vegetable oils from different plant sources vary in triglyceride compositions and unsaturation as summarized in Table 1. The unsaturation of unmodified vegetable oils ranges from 3.37 carbon-carbon double bonds per triglyceride molecule for peanut oil to 6.2 carbon-carbon double bonds for linseed oil. Vegetable oil compositions vary significantly depending on a wide range of factors, including environmental conditions and processing techniques.¹⁹ Additionally, unsaturation measurements based on ¹H NMR spectral analysis can differ slightly from values reported based on other analytical techniques.²⁰

Table 1. Triglyceride composition and unsaturation of selected vegetable oils

Vegetable Oil	Double bonds ^a	Fatty Acid Composition (%)					
		Palmitic C16:0	Stearic C18:0	Oleic C18:1	Linoleic C18:2	Linolenic C18:3	Ricinoleic C18:1
Peanut ^b	3.37	11.1	2.4	46.7	32	–	–
Corn ^b	4.45	10.9	2	25.4	59.6	1.2	–
Soybean ^b	4.61	10.6	4	23.3	53.7	7.6	–
Castor ^c	3.04	1	1	3	4.2	–	89
Linseed ^b	6.24	5.4	3.5	19	24	47	–

^a Average number of double bonds per triglyceride. ^b Taken from Ref [19]. ^c Taken from Ref [20].

All vegetable oil polyols for this study were prepared with a hydroxyl functionality of approximately 2.7 OH groups per molecule, because this value affords a good range of

residual unsaturation in the resulting polyols (0.4 to 3.5 carbon-carbon double bonds per molecule). In addition, this specific hydroxyl functionality enables a direct comparison with castor oil, which has a natural hydroxyl functionality of 2.7. Castor oil is comprised primarily of ricinoleic acid (> 89%), which contains a hydroxyl group at the C-12 position and a carbon-carbon double bond between C-9 and C-10.²¹ The structure of ricinolein, the major triglyceride of castor oil, is shown in Figure 1.

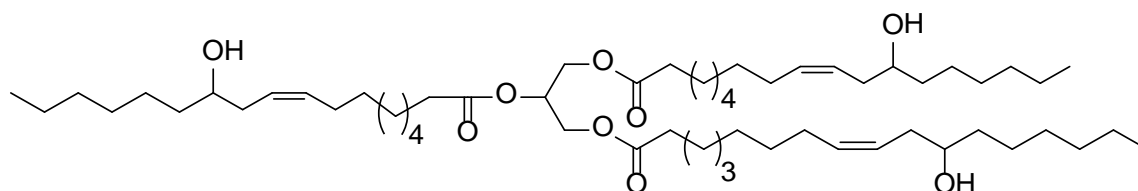


Figure 1. Ricinolein, major component of castor oil

Hydroxyl functionality, which is the number of hydroxyl groups per molecule, can be calculated by dividing the molecular weight of the polyol by its equivalent weight as shown in the following equation:

$$\text{Functionality} = \frac{\text{Molecular Weight}}{\text{Equivalent Weight}}$$

Equivalent weight is related to the hydroxyl number as shown in the equation below:

$$\text{Equivalent Weight} = \frac{56,100}{\text{OH Number}}$$

The hydroxyl numbers of polyols are values experimentally determined by acetylating the hydroxyl groups and titrating with potassium hydroxide.²² Hydroxyl numbers are defined by the mass of KOH in milligrams that is equivalent to the hydroxyl content of one gram of polyol.²² Substituting the expression for equivalent weight into the first

equation yields the following relationship for functionality in terms of molecular weight and hydroxyl number:

$$\text{Functionality} = \frac{\text{Molecular Weight} * \text{OH Number}}{56,100}$$

There are two major reasons why the effect of unsaturation has not been isolated in previous studies. First, controlling the partial epoxidation and subsequent ring opening of the oils to achieve the desired hydroxyl functionality with residual unsaturation is difficult. In practice, completely epoxidizing the vegetable oil and partially ring opening the oxirane groups is much easier. This limitation can be overcome by controlling the extent of partial epoxidation by adjusting the molar ratio of hydrogen peroxide to carbon-carbon double bonds.¹⁷ Second, it is difficult to accurately determine molecular weights. Typically, molecular weights are determined using size exclusion chromatography (SEC), light scattering, osmometry, or viscometry. However, each technique comes with significant drawbacks. Although SEC is the most common technique for determining the molecular weight of polymers, it is not an absolute method and is often inaccurate without a well characterized calibration standard.²³ There may also be problems with sample aggregation and adsorption onto column materials.²⁴ Although light scattering is a direct method for determining mass average molecular weight, it is a difficult, expensive, time-consuming procedure and does not provide information about polydispersity.²⁵ Likewise, osmometry is a direct, but time-consuming method for determining number average molecular weights that does not provide information about polydispersity.²⁵

In the present study, matrix-assisted laser desorption/ionization time-of-flight mass spectrometry (MALDI-TOF) has been used to accurately determine the molecular weight and mass distribution of the vegetable oil polyols. MALDI-TOF is generally used to characterize

large biomolecules and synthetic polymers.^{26,27} MALDI-TOF overcomes two significant challenges encountered with other mass spectrometry techniques used to measure the molecular weight of large molecules: low volatility that makes it difficult to evaporate large molecules and thermal stresses causing large molecules to break apart. MALDI is a soft ionization method and the mass spectra produced have minimal fragment-ion content.²⁸ With this technique, the sample is first dissolved in a solvent and then mixed with a solution containing small organic molecules that readily absorb UV laser light, called the matrix. This solution is subsequently dried to yield an analyte-doped matrix. Under laser irradiation, the top layer of the matrix undergoes desorption, carrying the analyte with it. The sample is then ionized and subsequently measured with a time-of-flight mass analyzer.²⁹ A previous study determined that dihydroxybenzoic acid (DHB) in acetone is the best matrix for vegetable oils.³⁰ For most biomolecules, the DHB matrix can serve as both a desorption and an ionization vehicle with the best overall performance at the intrinsic pH of the matrix. Thus, for the analysis of biomolecules with a DHB matrix, metal cationization agents are not always needed.^{23,31}

Although, MALDI provides accurate, direct molecular weight and weight distribution measurements, it does so only for polymer samples with a polydispersity index (PDI) below 1.1.^{32,33} If the PDI is higher (> 1.1), molecular weight measurements produce serious errors, because the assumption of constancy of intensity scale calibration is no longer valid.³⁴ To overcome this problem, polydisperse polymer samples have been grouped into monodisperse fractions using SEC, allowing the utilization of MALDI-TOF to calibrate the SEC curves.³⁵

Increasing the carbon-carbon double bond content may produce stiffer and stronger polymers and the present work indicates that residual unsaturation can significantly impact the physical and mechanical properties of the resulting polyurethane dispersions. Residual unsaturation is a variable that has not been considered in previous research when introducing different functionalities (*i.e.*, different OH number) into polyols from a single vegetable oil source. A second purpose of this research was to isolate the effect of different ring opening methods, while keeping the functionality and residual unsaturation constant. A previous study examined the effect of oxirane ring opening using different methods and reagents (hydrogen, methanol, hydrochloric acid, and hydrobromic acid); however, the OH functionality was not held constant, but ranged from 3.5 to 4.1 with minimal residual unsaturation.³⁶ In the present study, the range of OH functionality is much smaller (2.6 to 2.7). In addition, different chemicals (methanol, butanol, acetic acid, and hydrochloric acid) have been used for the oxirane ring opening.

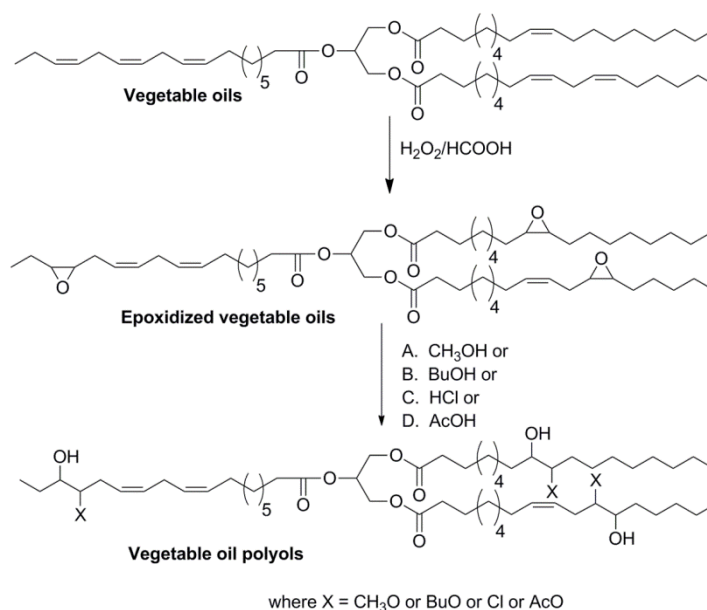
This is the first systematic attempt to isolate the effects of residual unsaturation in vegetable oil polyols on the properties of the resulting polyurethane coatings. While residual unsaturation is often considered undesirable, because it may lead to yellowing of the films, unsaturation from various sources (aromatic diisocyanates, alkyd resins, or castor oil) is fairly common in polyurethane coatings and some yellowing is tolerated in many applications. Residual unsaturation can also act as a site for further chemical modifications. In one previous study, grafted hybrid latexes were prepared by graft copolymerization of acrylic monomers onto polyurethanes made with partially epoxidized and ring-opened soybean oil. The residual carbon-carbon double bonds in the fatty acid chains were used as

graft sites.³⁷ Electron beam irradiation was used to crosslink residual carbon-carbon double bonds in vegetable oil-based polymers.³⁸

Experimental

Materials. Soybean oil, peanut oil, and corn oil were purchased at the local supermarket and used as received. Linseed oil was provided by Archer Daniels Midland Company (Decatur, IL, USA). Castor oil, dimethylol propionic acid (DMPA), isophorone diisocyanate (IPDI), and dibutyltin dilaurate (DBTDL) were purchased from Sigma-Aldrich (Milwaukee, WI, USA). Acetone, formic acid, glacial acetic acid, hydrogen peroxide, and methyl ethyl ketone (MEK) were purchased from Fisher Scientific Company (Fair Lawn, NJ, USA). All materials were used as received.

Synthesis of Vegetable Oil-Based Polyols. Various vegetable oils (peanut, corn, soybean, and linseed) were partially epoxidized using hydrogen peroxide and formic acid and subsequently ring opened to form polyols as illustrated in Scheme 1.



Scheme 1. Synthesis of vegetable oil-based polyols with residual unsaturation

The procedure used for epoxidation of the vegetable oils followed previously reported protocols.¹⁷ The relative amount of epoxidation was controlled by slightly adjusting the molar ratios of hydrogen peroxide. For more unsaturated oils, such as linseed oil, less hydrogen peroxide was needed. Generally, 250 g of vegetable oil, 85 to 100 g of hydrogen peroxide (30%) and 38 g of formic acid (88% in water) were added to a round bottom flask with a mechanical stirrer. The mixture was stirred in a water bath at 25 °C for 21 h. For the work-up, the epoxidized vegetable oil was washed with ethyl acetate and aqueous sodium chloride solution. The epoxidized vegetable oil was neutralized to a neutral pH with sodium bicarbonate and dried over anhydrous magnesium sulfate. The epoxidized vegetable oil was vacuum filtered, submitted to rotary evaporation at 38 °C for 1 h and dried in a 70 °C drying oven overnight. The oxirane content of the epoxidized vegetable oils was approximately 2.7 oxirane units per triglyceride, as determined by ¹H NMR spectroscopy.

The epoxidized oils were ring opened to prepare polyols with an approximate hydroxyl functionality of 2.7. Two different series of vegetable oil polyols were prepared. In the first series, different methoxylated vegetable oil polyols were synthesized from epoxidized oils. For ring opening with methanol, 246 g of epoxidized vegetable oil, 246 g of methanol, 246 g of isopropanol, and 10 g of fluoroboric acid were added to a 2 L round bottom flask. The mixture was stirred with a mechanical stirrer in a 45 °C mineral oil bath for 2 h. The reaction was quenched with aqueous ammonium hydroxide. For work-up, the sample was washed with ethyl acetate and aqueous sodium chloride solution. The methoxylated polyol was neutralized to a neutral pH with sodium bicarbonate and dried over anhydrous magnesium sulfate. The methoxylated polyol was vacuum filtered, submitted to rotary evaporation at 38 °C for 1 h and dried in a 70 °C drying oven overnight.

In the second series, several chemicals (methanol, butanol, hydrochloric acid, and acetic acid) were used to ring open epoxidized soybean oil (ESO) following previously described procedures.^{36,39} For ring opening with butanol, 60 g of ESO, 120 g of 1-butanol, and 2.5 g of fluoroboric acid were added to a round bottom flask. The mixture was stirred with a mechanical stirrer in a 45 °C mineral oil bath for 4 h. The reaction was quenched with aqueous ammonium hydroxide and the work-up followed the same procedures used for methoxylated polyols. For ring opening with hydrochloric acid, 247 g of ESO, 86 g of hydrochloric acid, and 300 mL of acetone were added to a round bottom flask. The mixture was stirred with a mechanical stirrer in a mineral oil bath at 40 °C for 2 h. The work-up followed the same procedures used for methoxylated polyols. Ring opening with acetic acid was achieved using a large excess of acetic acid relative to the ESO. Here, 40 g of ESO and 120 g of acetic acid were added to a two-neck flask with a reflux condenser and mechanical stirrer. The mixture was stirred in an 80 °C mineral oil bath for 8 h. Work-up followed the same procedures used for methoxylated polyols.

Synthesis of Vegetable Oil-Based Dispersions. The vegetable oil polyol, IPDI, DMPA, and one drop of DBTDL were added to a two-neck flask equipped with a mechanical stirrer. The molar ratios of OH groups from the vegetable oil polyol, NCO groups from the IPDI, and OH groups from the DMPA were kept at 1.0 : 1.7 : 0.69. As is customary in the preparation of polyurethane dispersions, an excess of diisocyanate was used, which can also react with the water. The diol, DMPA, acted as both a chain extender, increasing the molecular weight, and as an ionomer to promote dispersion. Steric hindrance prevented the carboxylic acid group in the DMPA from reacting with the isocyanate.⁵

Characterization. MALDI-TOF spectra were obtained using an Applied Biosystems Voyager DE Pro. The samples were diluted in acetone and a 10 mg/mL solution of 2,5-dihydroxybenzoic acid (DHB) in acetone was used as the matrix. The molecular weights were calculated based on procedures described in ASTM D7134, the standard for determining the molecular weight of atactic polystyrene using MALDI-TOF.³⁴ Minor modifications to the protocol were necessary to adapt the standard for use with vegetable oil polyols. Instead of all-*trans* retinoic acid, DHB was used for the matrix, which eliminated the use of silver salts. Acetone replaced tetrahydrofuran or toluene as the solvent.

The oxirane content and degree of unsaturation (carbon-carbon double bonds) were determined using ¹H NMR spectroscopy with a Varian Unity spectrometer at 300 MHz, as described previously in the literature.²⁰ The hydroxyl number was determined by following ASTM D1957.⁴⁰ The tensile properties were measured using an Instron universal testing machine (Model-4502). The crosshead speed was set at 100 mm/min. The average stress-strain data from five rectangular specimens (50 mm × 10 mm) were used. A dynamic mechanical analyzer (TA Instruments DMA Q800, New Castle, DE) in tensile mode at 1 Hz was used to determine the storage and loss moduli. The samples were heated from -80 to 100 °C at a rate of 5 °C/min. Differential scanning calorimetry (DSC) was performed using a differential scanning calorimeter (TA Instruments DSC Q20, USA). The samples were heated from 25 to 100 °C at a rate of 20 °C/min to erase their thermal history, cooled to -70 °C, and heated again to 150 °C at a heating rate of 20 °C/min. The sample masses were approximately 5 mg. A thermogravimetric analyzer (TA Instruments TGA Q50, USA) was used to measure the weight loss of the polyurethane films in an air atmosphere. The samples

were heated from 30 to 650 °C at a heating rate of 20 °C/min. The mass of the samples used for TGA analysis was approximately 8 mg.

Results and Discussion

Polyol Characterization. The vegetable oil polyols exhibited narrow molecular weight distributions with low PDI values (< 1.1), which allowed for quantitative molecular weight characterization by MALDI-TOF. A representative MALDI-TOF spectrum is shown in Figure 2. The number average, M_n , and mass average, M_w , molecular weights were calculated from the peak intensity and centroid mass results based on methods described in ASTM D7134. Corrections for baseline noise were made based on the recommended signal to noise ratio (S/N) of 3:1.

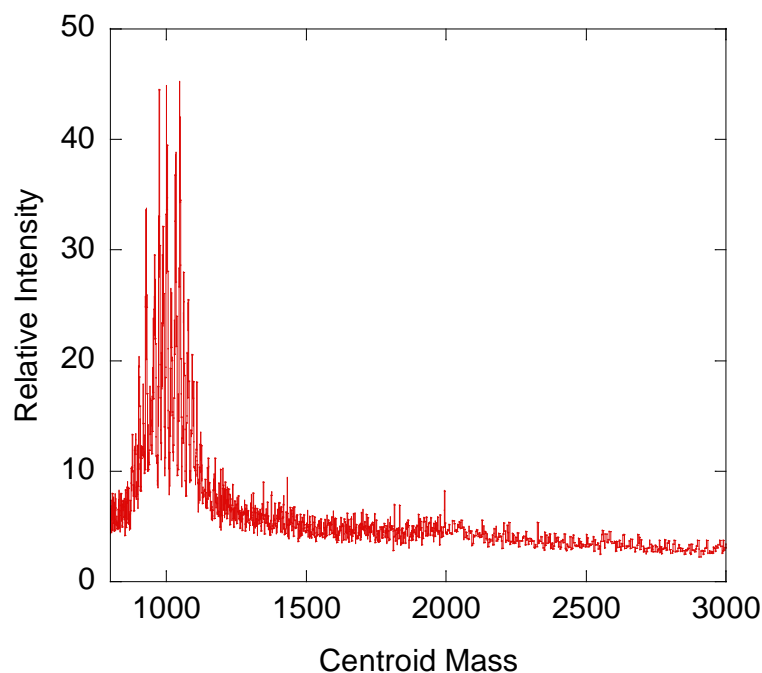


Figure 2. MALDI-TOF spectrum of methoxylated soybean oil polyol

The molecular weights for the modified vegetable oil polyols ranged from 1030 to 1226 g/mol. Castor oil, a natural polyol, had a molecular weight of 933 g/mol, which corresponds to the structure of ricinolein, the triglyceride of ricinoleic acid. It should be noted that the higher average molecular weight and slightly higher PDI of the soybean polyol ring opened by acetic acid was likely caused by dimerization of two triglycerides. This may occur when a hydroxyl group formed during a previous ring opening step is involved in the ring opening of an oxirane group on a second triglyceride molecule. However, the extent of dimerization was minimized by using an excessive amount of acetic acid, as evidenced by the resulting PDI below 1.1.

The results for the residual degree of unsaturation, molecular weight, and OH functionality are listed in Table 2. Based on the ^1H NMR spectroscopic results, the residual unsaturation per molecule ranged from 0.4 for the peanut oil-based polyol to 3.5 for the linseed oil-based polyol. The corn oil-based polyol and soybean oil-based polyol exhibited similar amounts of residual unsaturation (1.3 and 1.6, respectively). All polyols under investigation had an approximate hydroxyl functionality of 2.7 OH groups per molecule.

Table 2. Properties of vegetable oil-based polyols

Polyol	OH Functionality	Deg. of Unsat.	OH Number	M_n	PDI
Peanut - MeOH	2.7	0.4	139	1072	1.03
Corn - MeOH	2.6	1.3	143	1030	1.01
Soybean - MeOH	2.7	1.6	142	1067	1.02
Castor	2.7	3.1	163	933	1.01
Linseed - MeOH	2.8	3.5	147	1076	1.02

Polyol	Functionality	Deg. Of Unsat.	OH Number	M_n	PDI
Soybean - MeOH	2.7	1.6	142	1067	1.02
Soybean - AcOH	2.7	1.6	123	1226	1.06
Soybean-HCl	2.6	1.3	136	1054	1.01
Soybean - BuOH	2.7	1.8	139	1092	1.01

Tensile Properties. The stress-strain curves for polyurethane films prepared with different vegetable oils are shown in Figure 3. The modulus and toughness increase with higher unsaturation, while the % strain decreases. It should also be noted that castor oil behaves differently than the other vegetable oils, which is attributed to the different triglyceride composition found in castor oil. Because castor oil primarily consists of ricinolein, the hydroxyl groups are uniformly positioned at the 12th carbon in the chain. Therefore, castor oil has a very homogenous distribution of hydroxyl functional groups compared to polyols prepared from various other epoxidized vegetable oils.

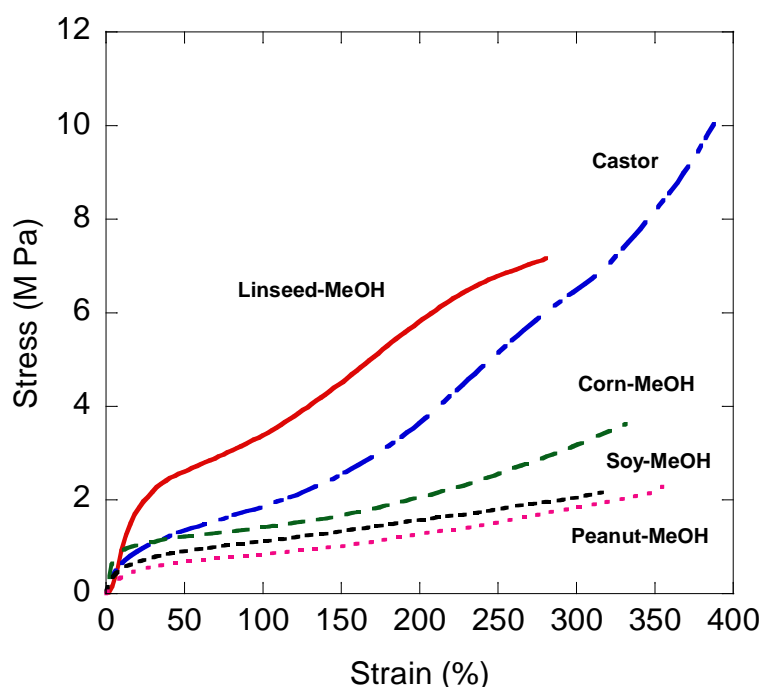


Figure 3. Stress-strain curves for polyurethane films from different vegetable oil polyols

The stress-strain curves for polyurethane films prepared from epoxidized soybean oils by different ring opening methods are shown in Figure 4. The ring opening with hydrochloric acid and acetic acid produced stronger films with a higher Young's modulus, break strength,

and % strain compared to films produced by ring opening with methanol. Ring opening with 1-butanol made the films softer by significantly lowering their toughness compared to films produced by ring opening with methanol. The tensile properties for films prepared from both different vegetable oils and with different ring opening methods are summarized in Table 3.

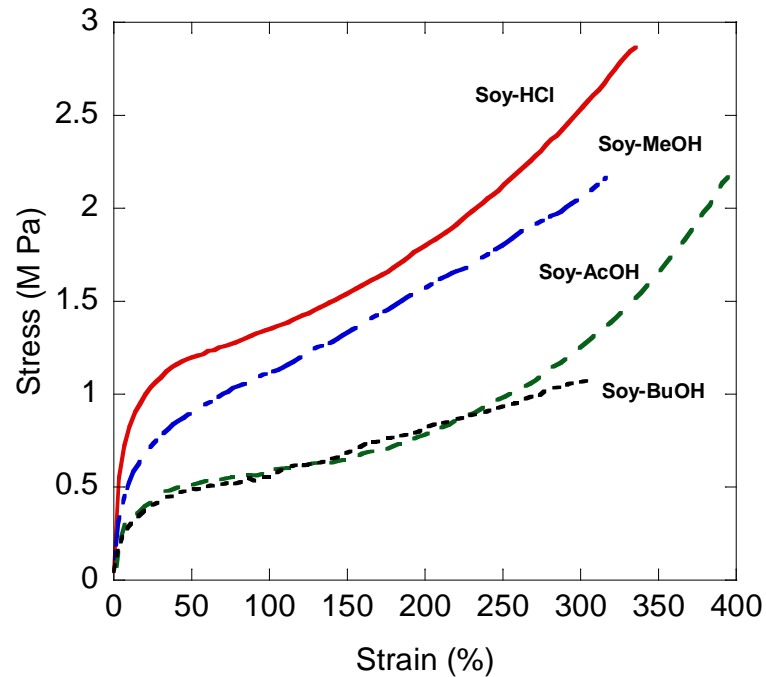


Figure 4. Stress-strain curves for polyurethane films from soybean polyols created by different ring opening methods

Table 3. Summary of engineering stress data

Polyol	Break Strength (MPa)	Young's Modulus (MPa)	Toughness (MPa)	% Strain
Peanut-MeOH	2.27 ± 0.03	4.64 ± 1.09	4.25 ± 0.12	343 ± 10
Corn-MeOH	3.40 ± 0.23	12.77 ± 0.83	6.02 ± 0.40	322 ± 12
Soybean-MeOH	2.14 ± 0.06	5.20 ± 0.16	4.11 ± 0.18	312 ± 5
Castor	10.61 ± 1.91	6.29 ± 0.54	15.26 ± 3.54	363 ± 39
Linseed-MeOH	7.55 ± 0.54	16.15 ± 2.13	12.72 ± 1.06	280 ± 14

Polyol	Break Strength (MPa)	Young's Modulus (MPa)	Toughness (MPa)	% Strain
Soybean-MeOH	2.14 ± 0.06	5.20 ± 0.16	4.11 ± 0.18	312 ± 5
Soybean-AcOH	2.19 ± 0.33	4.81 ± 0.16	3.80 ± 0.49	392 ± 26
Soybean-HCl	2.76 ± 0.28	15.23 ± 2.19	5.60 ± 0.59	338 ± 17
Soybean-BuOH	1.13 ± 0.08	3.54 ± 0.45	2.24 ± 0.13	312 ± 11

Dynamic Mechanical Analysis (Kinetic Transition). Figure 5 shows the storage modulus as a function of temperature for films prepared from different vegetable oils. The drop in storage modulus generally shifted to higher temperatures with higher amounts of residual carbon-carbon double bonds. A sharper drop in storage modulus for the film based on castor oil compared to the other films can be attributed to the more homogeneous distribution of the hydroxyl groups in castor oil compared to the other vegetable oils.

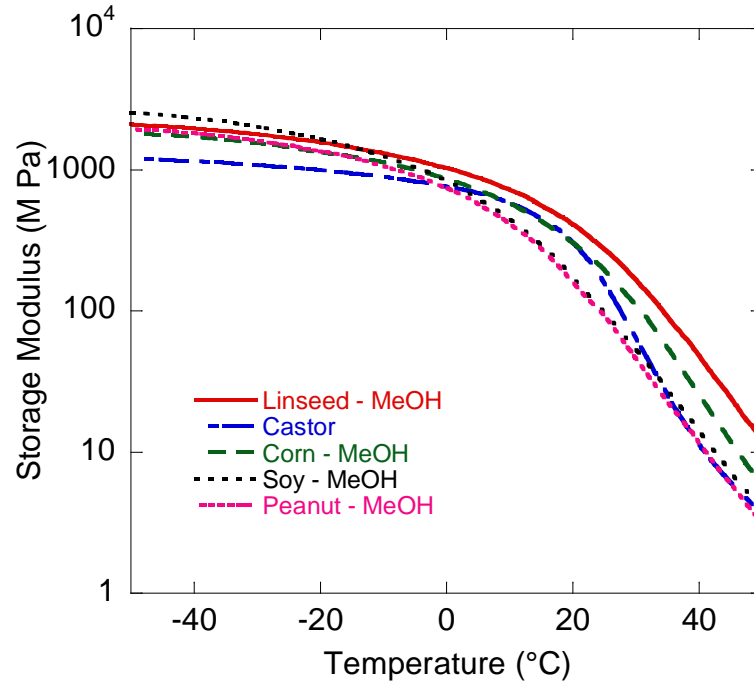


Figure 5: Storage modulus as a function of temperature for polyurethane films from different vegetable oil polyols

Figure 6 shows the storage modulus as a function of temperature for soybean polyol films with different side groups. Both the storage modulus and the temperature at which the storage modulus dropped increased in the following order of the side groups: 1-butanol < acetic acid, methanol < hydrochloric acid.

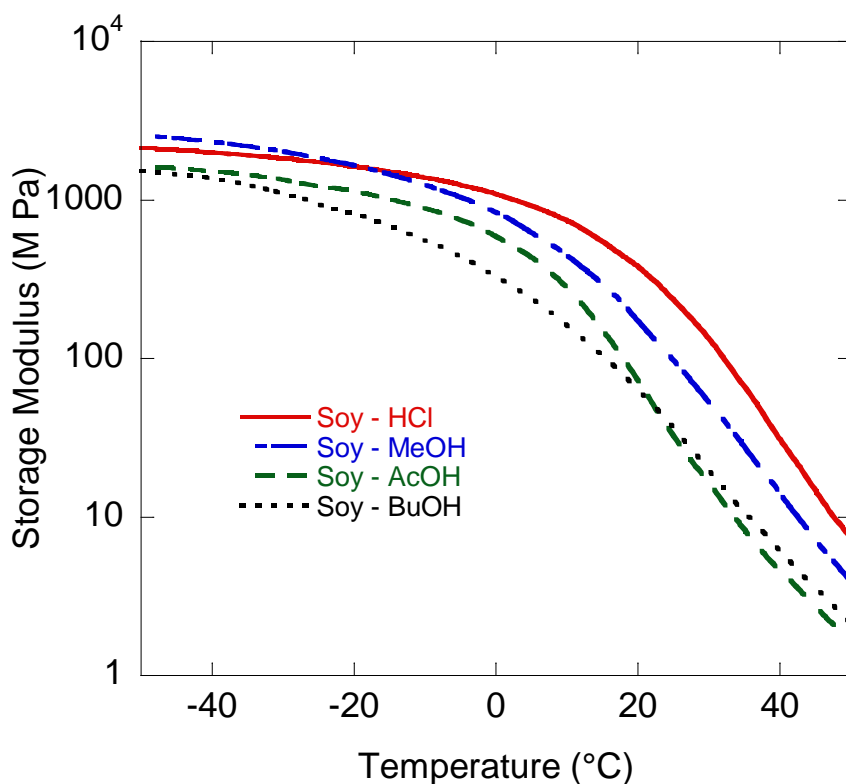


Figure 6: Storage modulus as a function of temperature for polyurethane films from soybean polyols created by different ring opening methods

Differential Scanning Calorimetry (Glass Transition Temperature). The glass transition temperatures (T_g) of the polyurethane films were determined by DSC and are listed in Table 4. For films prepared from different vegetable oil polyols, the T_g increased with increasing carbon-carbon double bond content. However, the slight variation between the films prepared with methoxylated soybean oil polyol ($T_g = -7.9$ °C) and with methoxylated corn oil polyol ($T_g = -6.6$ °C) are attributed to possible differences in triglyceride composition. Based on the overall trend of increasing T_g with increasing unsaturation, the films prepared from soybean oil polyol should have had a slightly higher T_g than those prepared from the corn oil polyol.

The side chains formed by different ring opening methods have a significant effect on the T_g . Substituting a longer butoxy side chain for the methoxy group lowered the T_g from -7.9 °C to -26.6 °C. Changing the methoxy group to an acetoxy group raised the T_g from -7.9 °C to 3.4 °C, and changing to a chloro group raised the T_g to 2.9 °C.

Table 4. Glass transition temperatures of polyurethane films based on DSC thermograms

Polyol	Deg. of Unsat. per Polyol	T_g (°C)
Peanut - MeOH	0.4	-9.2
Corn - MeOH	1.3	-6.6
Soybean - MeOH	1.6	-7.9
Castor	3.1	6.8
Linseed - MeOH	3.5	13.5

Polyol	Deg. of Unsat. per Polyol	T_g (°C)
Soybean - BuOH	1.8	-26.6
Soybean - MeOH	1.6	-7.9
Soybean - HCl	1.3	2.9
Soybean - AcOH	1.6	3.4

Thermogravimetric Analysis. The thermograms for films prepared from different vegetable oil polyols are shown in Figure 7. They show that the higher number of residual carbon-carbon double bonds in the linseed polyol decreased the thermal stability at lower temperatures; however, this effect was reversed at higher temperatures.

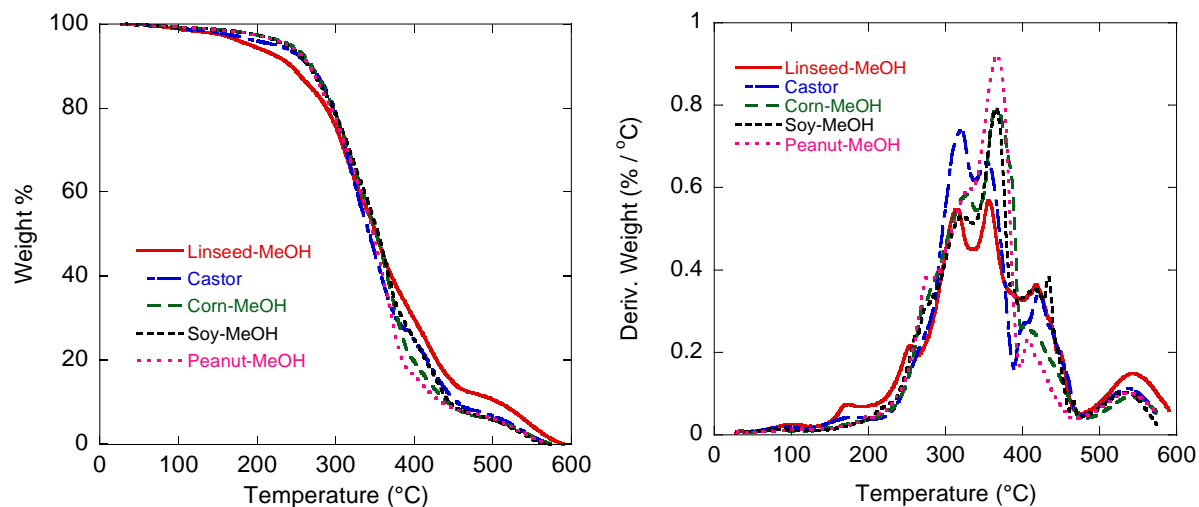


Figure 7. TGA curves for polyurethane films from different vegetable oil polyols

The thermograms for films prepared from soybean polyols by different ring opening methods are shown in Figure 8. The films made from soybean polyols by acid ring opening (acetic and hydrochloric acids) exhibited lower thermal stabilities at temperatures below 350 °C. However, at higher temperatures the film prepared from soybean polyol by hydrochloric acid ring opening was more thermally stable than the other polyols.

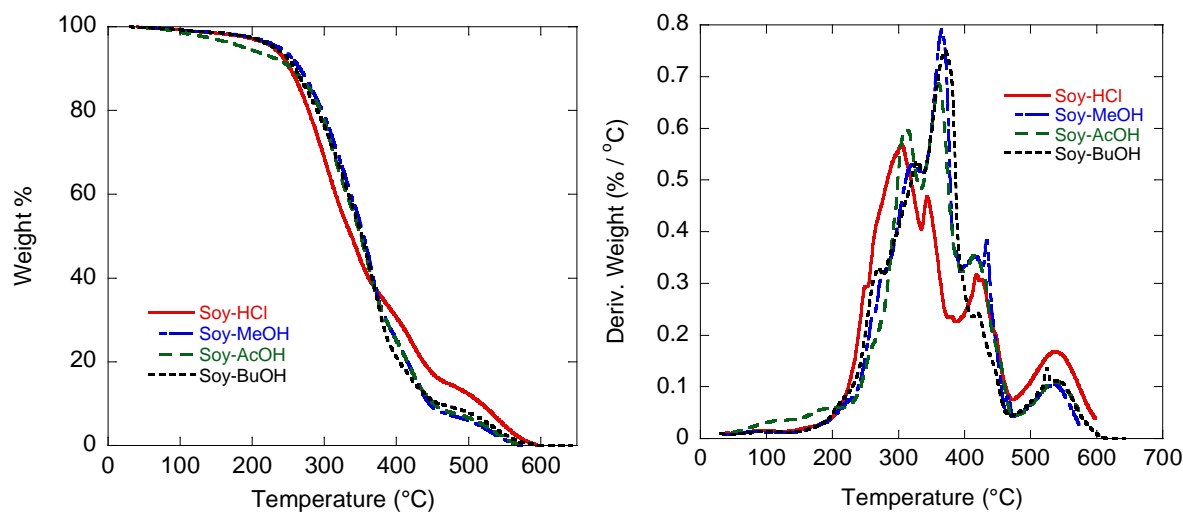


Figure 8: TGA curves for polyurethane films from soybean polyols created by different ring opening methods

Conclusions

Residual unsaturation has a strong influence on the mechanical and thermal properties of specific bio-based polyurethane films. Higher amounts of residual unsaturation led to increases in mechanical properties, such as modulus, which increased from 4.64 to 16.15 MPa; the toughness increased from 4.25 to 12.72 MPa; and the break strength increased from 2.27 to 7.55 MPa, when changing from a peanut oil-based polyol to a linseed oil-based polyol. Correspondingly, decreases in the % strain at break from 343% to 280% were observed. The glass transition temperatures observed by DSC increased from -9.2 to 13.5 °C.

This investigation indicates that the fatty acid composition also plays an important role. Saturated fatty acid chains and fatty acid chains whose carbon-carbon double bonds are not converted into ring opened oxiranes become dangling chains in the polyurethane films and act as plasticizers. Castor oil-based polyurethane films exhibit different physical properties. In comparison to linseed oil, the castor oil-based films exhibit higher break strength (10.61 MPa) and toughness (15.26 MPa). Conversely, the castor oil-based polyurethane films exhibit higher % strain at break (363%) than polyurethane films made with peanut oil-based polyol. The differences in physical properties of castor oil-based polyurethane films and other films based on vegetable oil polyols can be attributed to the more homogenous distribution of hydroxyl groups in castor oil caused by its composition (> 89% ricinoleic acid).

The inconsistent results seen for similar unsaturated oils (corn and soybean) may in part be explained by the minor differences in the compositions of the two oils. Corn oil has more oleic acid (one carbon-carbon double bond) and less linolenic acid (three carbon-carbon

double bonds) than soybean oil, which render corn oil-based polyols less likely to have two ring opened oxiranes on a single fatty acid chain and more likely to have fatty acid chains without a single hydroxyl group compared to soybean oil-based polyols.

Our study of soybean polyols prepared by different oxirane ring opening methods (methanol, butanol, acetic acid, and hydrochloric acid) indicates that the method of ring opening impacts the resulting properties of the polyurethane films. In particular, increasing the alcohol chain length (methanol vs. butanol) decreases the break strength from 2.14 to 1.13 MPa, the toughness from 4.11 to 2.24 MPa, and the T_g from -7.9 to -26.6 °C. Ring opening with hydrochloric acid results in polyurethane films with higher Young's modulus than polyurethane films created by other ring opening methods, whereas ring opening with acetic acid affords a film with a higher T_g .

Acknowledgements

We gratefully acknowledge financial support from the Consortium for Plant Biotechnology Research (CPBR) and the Archer Daniels Midland (ADM) Company. We also thank Mr. Joel Nott and Ms. Margie Carter of the Protein Facility at Iowa State University for their assistance with the MALDI-TOF measurements.

References

1. R. B. Seymour and G. B. Kauffman, *J. Chem. Educ.*, 1992, **69**, 909.
2. R. Amari, *Paint Manufacturing in the US*, IBISWorld Inc., 2012.
3. U. Meier-Westhues, *Polyurethanes - Coatings, Adhesives and Sealants*, Vincentz Network, Hannover, Germany, 2007.
4. K. D. Weiss, *Prog. Polym. Sci.*, 1997, **22**, 203.
5. Z. W. Wicks, Jr., F. N. Jones, S. P. Pappas and D. A. Wicks, *Organic Coatings: Science and Technology*, John Wiley & Sons, Inc., Hoboken, NJ, 2007.
6. B. K. Kim, *Colloid Polym. Sci.*, 1996, **274**, 599.
7. J. Bourne, *Surf. Coat. Int.*, 2009, **92**, 244.
8. D. L. Greene, J. L. Hopson and J. Li, *Energ. Policy*, 2006, **34**, 515.

9. D. Fantazzini, M. Höök and A. Angelantoni, *Energ. Policy*, 2011, **39**, 7865.
10. International Energy Agency, *World Energy Outlook 2012*, Paris, France, 2012.
11. Ø. Harsem, A. Eide and K. Heen, *Energ. Policy*, 2011, **39**, 8037.
12. U.S. Department of Energy, *Annual Energy Outlook 2012 with Projections to 2035*, Washington, DC, 2012.
13. Y. Lu and R. C. Larock, in *Green Polymer Chemistry: Biocatalysis and Biomaterials*, American Chemical Society, 2010, vol. 1043, pp. 87-102.
14. Y. Xia and R. C. Larock, *Green Chem.*, 2010, **12**, 1893.
15. Z. S. Petrovic, *Polym. Rev.*, 2008, **48**, 109.
16. V. D. Athawale and R. V. Nimbalkar, *J. Disper. Sci. Technol.*, 2011, **32**, 1014.
17. Y. Lu and R. C. Larock, *Biomacromolecules*, 2008, **9**, 3332.
18. A. Zlatanić, C. Lava, W. Zhang and Z. S. Petrović, *J. Polym. Sci. Pol. Phys.*, 2004, **42**, 809.
19. M. A. R. Meier, J. O. Metzger and U. S. Schubert, *Chem. Soc. Rev.*, 2007, **36**, 1788.
20. D. D. Andjelkovic, M. Valverde, P. Henna, F. Li and R. C. Larock, *Polymer*, 2005, **46**, 9674.
21. D. S. Ogunniyi, *Bioresour. Technol.*, 2006, **97**, 1086.
22. E. Marengo, M. Bobba, E. Robotti and M. Lenti, *Anal. Chim. Acta*, 2004, **511**, 313.
23. H. Pasch and W. Schrepp, *MALDI-TOF Mass Spectrometry of Synthetic Polymers*, Springer, Berlin, 2003.
24. G. Klärner, C. Former, K. Martin, J. Räder and K. Müllen, *Macromolecules*, 1998, **31**, 3571.
25. J. R. Fried, *Polymer Science & Technology*, Prentice Hall Professional Technical Reference, Upper Saddle River, NJ, 2003.
26. H. Räder and W. Schrepp, *Acta Polym.*, 1998, **49**, 272.
27. A. Marie, F. Fournier and J. C. Tabet, *Anal. Chem.*, 2000, **72**, 5106.
28. C. A. Jackson and W. J. Simonsick Jr, *Curr. Opin. Solid St. M.*, 1997, **2**, 661.
29. E. d. Hoffmann and V. Stroobant, *Mass Spectrometry: Principles and Applications.*, John Wiley & Sons Ltd, West Sussex, England, 2007.
30. G. R. Asbury, K. Al-Saad, W. F. Siems, R. M. Hannan and H. H. Hill, Jr., *J. Am. Soc. Mass Spectr.*, 1999, **10**, 983.
31. D. Dogruel, R. W. Nelson and P. Williams, *Rapid Commun. Mass Sp.*, 1996, **10**, 801.
32. M. W. F. Nielen and S. Malucha, *Rapid Commun. Mass Sp.*, 1997, **11**, 1194.
33. G. Montaudo, M. S. Montaudo, C. Puglisi and F. Samperi, *Rapid Commun. Mass Sp.*, 1995, **9**, 453.
34. ASTM International, Standard Test Method for Molecular Mass Averages and Molecular Mass Distribution of Atactic Polystyrene by Matrix Assisted Laser Desorption/Ionization (MALDI)-Time of Flight (TOF) Mass Spectrometry (MS), West Conshohocken, PA, 2005.
35. G. Montaudo, D. Garozzo, M. S. Montaudo, C. Puglisi and F. Samperi, *Macromolecules*, 1995, **28**, 7983.
36. A. Guo, Y. Cho and Z. S. Petrović, *J. Polym. Sci. Pol. Chem.*, 2000, **38**, 3900.
37. Y. Lu and R. C. Larock, *Biomacromolecules*, 2007, **8**, 3108.
38. M. Thunga, Y. Xia, U. Gohs, G. Heinrich, R. C. Larock and M. R. Kessler, *Macromol. Mater. Eng.*, 2012, **297**, 799.

39. F. A. Zaher, M. H. El-Mallah and M. M. El-Hefnawy, *J. Am. Oil Chem. Soc.*, 1989, **66**, 698.
40. ASTM International, Standard Test Method for Hydroxyl Value of Fatty Oils and Acids, West Conshohocken, PA, 2001.

CHAPTER 3. MECHANICAL AND ANTIBACTERIAL PROPERTIES OF SOYBEAN-OIL-BASED CATIONIC POLYURETHANE COATINGS: EFFECTS OF AMINE RATIO AND DEGREE OF CROSSLINKING

A paper submitted to *Biomacromolecules*

Authors: Thomas F. Garrison¹, Zongyu Zhang², Hyun-Joong Kim², Debjani Mitra², Ying Xia¹, Daniel P. Pfister¹, Byron F. Brehm-Stecher², Richard C. Larock*¹ and Michael R. Kessler*³

¹ Department of Chemistry, Iowa State University, Ames, Iowa

² Department of Food Science and Human Nutrition, Iowa State University, Ames, Iowa

³ Department of Materials Science and Engineering, Iowa State University, Ames, Iowa

Abstract

Soybean oil-based cationic polyurethane coatings with antibacterial properties have been prepared with different molar ratios of an amine diol and with soy polyols with different hydroxyl numbers. All of the cationic PU dispersions and films exhibit inhibitory activity against three foodborne pathogens: *Salmonella* Typhimurium, *Listeria monocytogenes*, and *Staphylococcus aureus*. It is generally observed that increases in the ratio of ammonium cations improve the antibacterial performance. Reduction of the crosslink density by decreasing the hydroxyl number of the soy polyol also results in slightly improved antibacterial properties. Higher glass transition temperatures and improved mechanical properties are observed with corresponding increases in the molar ratios of the amine diol and the diisocyanate. These results show that the mechanical properties of these coatings can be tuned, while maintaining good antibacterial activity.

Introduction

In the past few years, there has been an increased interest in the use of various agricultural commodities as biorenewable alternatives to petroleum for the synthesis of plastic materials.^{1,2} Long-term concerns about the cost and availability of petroleum supplies have been driving factors behind this push for sustainability.³ In particular, plant-based oils are commonly used as renewable raw materials as these are readily available, generally inexpensive, are biodegradable and have low toxicities, among other advantages.^{4,5}

Polyurethanes are especially amenable to use of biorenewable plant-based oils as raw materials.⁶ Polyurethanes comprise an important class of polymers and are used widely throughout industry in foams, coatings, adhesives and cast elastomers.⁷ In particular, waterborne polyurethane dispersions (PUDs) have garnered substantial interest as environmentally-friendly coatings.⁸⁻¹⁰ Waterborne PUDs have significant advantages over PUDs manufactured using traditional organic solvents. Specifically, aqueous systems are more cost effective than organic-based approaches and the use of water as a solvent reduces or even eliminates the emission of harmful volatile organic compounds.^{11,12} More recently, the development of waterborne PUDs made with biorenewable oils has become the focus of research into environmentally-friendly protective and/or decorative coatings.¹³⁻¹⁵

To date, anionic waterborne PUDs are more prevalent, both in industry and in the literature, than cationic PUDs.¹¹ Typically, anionic PUDs are prepared by incorporating a diol or polyol that also contains a carboxylic acid group, such as dimethylolpropionic acid (DMPA), into the polymer backbone. The PU is then neutralized with a tertiary amine such as triethylamine (TEA) and dispersed in water. Anionic polyurethane dispersions have been

successfully prepared using 50-60 wt% vegetable oil polyols.¹⁴ However, a key disadvantage of anionic PUDs is their lack of antimicrobial activity.

In contrast, cationic PUDs, which are prepared by incorporating a tertiary amine diol or polyol followed by treatment with an acid, are seldom used commercially. One potential advantage of cationic PUDs is that they have been found to exhibit excellent adhesion properties.^{11,16-18} However, the antimicrobial properties of cationic PUDs are of much greater interest.¹⁸ Cationic compounds are able to bind to bacteria and other microbes and disrupt cell structure, resulting in permeabilization and death. For example, other polymer coatings that contain amine groups, certain cationic peptides, and chitosan, which is a positively-charged carbohydrate polymer derived from crustacean shells, are all known to be antimicrobial.¹⁹ Recently, an aqueous coating using chitosan was reported; however, drawbacks of this technique include its complexity, the need for electrografting, and the limited solubility of chitosan.²⁰

Our group has previously reported novel cationic polyurethane dispersions from vegetable oil-based polyols.¹⁶ A further study from our group examined the effects of the hydroxyl functionality of the soybean oil-based polyols on the thermal and mechanical properties of cationic polyurethanes.¹⁷ We recently reported the first study on the effect of different polyols on the antibacterial properties of cationic plant-oil based PUDs and PU coatings.²¹ In the current work, environmentally-friendly, plant oil-based, cationic PUDs with excellent coating properties have been successfully synthesized from soybean oil-based polyols. We examined the effects of the molar ratio of the tertiary amine diol *N*-methyl diethanolamine (MDEA) used and the effects of crosslink density on the thermo-mechanical properties and antibacterial properties of PUDs and PU films. The antibacterial properties of

these materials have been evaluated using the disk diffusion assay against *Listeria monocytogenes* and *Salmonella enterica* serovar Typhimurium, the two most common causative agents of bacterial foodborne illnesses.^{22,23} We have also performed disk diffusion tests using methicillin-resistant *Staphylococcus aureus* (MRSA), which is resistant to antibiotics commonly used to treat staphylococcal infections. MRSA infection may occur after invasive surgical procedures, such as the implantation of a medical device (hospital-acquired MRSA) or as a topical infection through person-to-person transmission among those in close physical contact, such as wrestlers or care providers (community-acquired MRSA). A food-related route for transmission of MRSA has also been reported - a community-acquired outbreak of acute gastroenteritis that was traced to contamination of foods by an asymptomatic food worker.²⁴ Further, MRSA has been detected in raw meat samples (beef, pork, chicken, turkey) at levels ranging from 0.7% - 35.5%.²⁵ Together, these data indicate that food workers or the food supply could represent additional reservoirs for the transmission of MRSA.

The antibacterial properties of the cationic plant oil based PUDs and PU films examined here suggest their potential value as coatings for surfaces in food processing or healthcare environments or as elements in food packaging for pathogen control. Our results also indicate that the thermal and mechanical properties of these novel cationic PU films can be tuned, while maintaining their antibacterial properties.

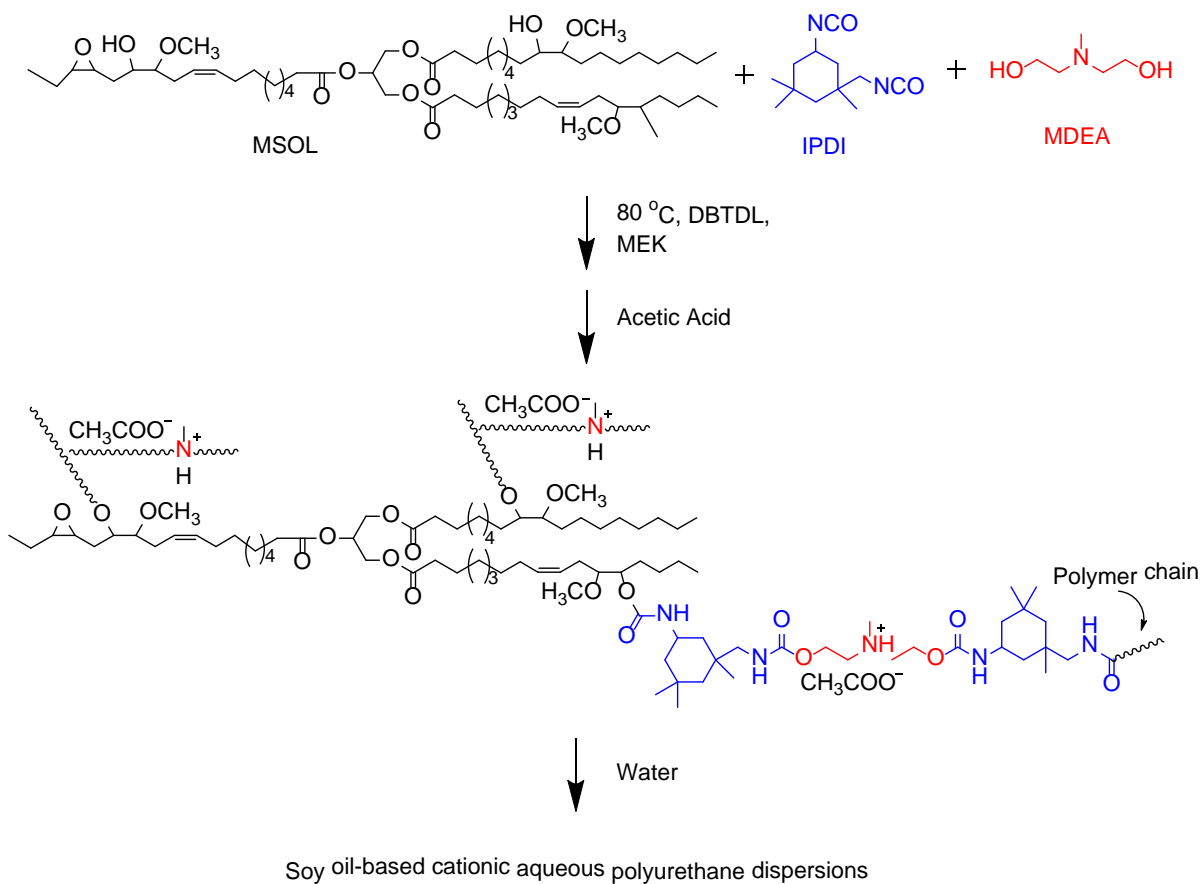
Experimental

Materials. Soybean oil was purchased at the local supermarket and used directly. Methoxylated soybean polyols (MSOL) with hydroxyl numbers of 140, 155, and 174 mg KOH/g were synthesized as previously reported.¹⁴ Dimethylolpropionic acid (DMPA), *N*-

methyl diethanolamine (MDEA), isophorone diisocyanate (IPDI), and dibutyltin dilaurate (DBTDL) were purchased from Aldrich Chemical Company (Milwaukee, WI, USA). Glacial acetic acid and methyl ethyl ketone (MEK) were purchased from Fisher Scientific Company (Fair Lawn, NJ, USA). All materials were used as received.

Synthesis of the Soybean Oil-based Cationic PUDs. The IPDI, MSOL, and MDEA were added to a three-necked flask equipped with a mechanical stirrer, condenser, and thermometer. The molar ratio of NCO groups from IPDI was varied from 2.0 to 2.75. The molar ratio of OH groups from MSOL was kept constant at 1.0, while the molar ratio of OH groups from MDEA varied from 0.95 to 1.7 (corresponding to the NCO molar ratio of IPDI). One drop of DBTDL was added to the reaction mixture. The reaction was first carried out at 80 °C for 10 minutes and then MEK (50 wt% based on the reactant) was added to reduce the viscosity. After 2 h reaction, the reactants were then cooled to room temperature and neutralized by the addition of 1.5 equivalents of acetic acid, followed by dispersion at high speed with distilled water to produce the cationic PUD with a solid content of about 12.5 wt% after removal of the MEK under vacuum. The corresponding PU films were obtained by drying the resulting dispersions at room temperature in polystyrene petri dishes. As a control to confirm the role of cationic charge in the PUD antibacterial activity, a plant oil-based anionic dispersion was prepared using DMPA as previously reported.¹⁴ The molar ratios for the anionic PUD control were 2.0 NCO from IPDI, 1.0 OH from MSOL, and 0.95 OH from DMPA. The chemical structure of the starting materials and a representative polymer structure are shown in Scheme 1. The nomenclature used for the various PUD samples and their composition is listed in Table 1, where the letter (A, B, or C) corresponds

to the MSOL hydroxyl number and the number (1, 2, or 3) corresponds to different molar ratios of IPDI and MDEA.



Scheme 1. Polymer structure of the cationic plant-oil based polyurethane

Table 1. Sample nomenclature and composition.

Sample Name	Polyol OH Number (mg KOH / g)	Molar Ratios of Functional Groups		
		OH Groups Polyol	OH Groups MDEA	NCO Groups (IPDI)
A1-AN ^a	140	1.00	0.95 ^b	2.00
A1	140	1.00	0.95	2.00
B1	155	1.00	0.95	2.00
B2	155	1.00	1.45	2.47
B3	155	1.00	1.70	2.75
C1	174	1.00	0.95	2.00

^a A1-AN: an anionic version of PUD A1, used as a control for the cationic nature of the PU antibacterial activity. ^b DMPA was used instead of MDEA

Thermal and Mechanical Analysis. The dynamic mechanical behavior of the PUDs was characterized using a dynamic mechanical analyzer (TA Instruments DMA Q800, New Castle, DE) in tensile mode at 1 Hz. The samples were heated from -70 to 100 °C at a rate of 5 °C/min. For this study, the glass transition temperatures (T_g) were determined from the onset temperatures of the decrease in storage modulus. Differential scanning calorimetry (DSC) was performed using a differential scanning calorimeter (TA Instruments DSC Q20, USA). The samples were heated from 25 to 80 °C at a rate of 20 °C/min to erase their thermal history, cooled to -70 °C, and heated again to 100 °C at a heating rate of 20 °C/min. The sample mass was approximately 4 mg. A thermogravimetric analyzer (TA Instruments TGA Q50, USA) was used to measure the weight loss of the PUDs in an air atmosphere. The samples were heated from 30 to 650 °C at a heating rate of 20 °C/min. The mass of the samples used for TGA analysis was approximately 8 mg.

Bacterial Strains and Growth Conditions. The test cultures, *Salmonella enterica* serovar Typhimurium ATCC 13311 and *Staphylococcus aureus* ATCC BAA-44 (methicillin-resistant) were acquired from the American Type Culture Collection (ATCC, Manassas, VA, USA). *Listeria monocytogenes* NADC 2045 was from the USDA National Animal Disease Center (NADC, Ames, IA). Cultures were maintained as frozen stocks at $-80\text{ }^{\circ}\text{C}$ in Tryptic Soy Broth (TSB, BD Diagnostics Systems, Sparks, MD) containing 20% (v/v) glycerol. Working cultures of these bacteria were maintained on Tryptic Soy Agar (TSA) plates. Strains were grown in TSB for 18 h at $35\text{ }^{\circ}\text{C}$ and the optical densities of the resulting bacterial cultures were measured spectrophotometrically (model DU720, Beckman Coulter). The relationship between absorbance at 600 nm (A_{600}) and plate counts was determined for cultures adjusted to A_{600} values of 0.1 (10^8 CFU mL^{-1}) or 1.0 (10^9 CFU mL^{-1}) using fresh TSB. This relationship was used in subsequent experiments to prepare working bacterial suspensions in TSB or 0.85% saline containing 10^6 CFU mL^{-1} (for disk diffusion tests) or 10^5 CFU mL^{-1} (for Bioscreen and PU film leaching tests).

Antibacterial Testing. *Disk diffusion tests.* The antibacterial properties of both PU dispersions and dried films cast onto sterile paper disks (polymer-fiber composites) were examined against all three test organisms, as described previously, using Clinical and Laboratory Standards Institute (CLSI) methods.²¹

Additional testing with S. Typhimurium. To obtain more detailed information on the relative efficacy and mechanism of action for select PU films, further testing was performed beyond the initial disk diffusion work using *S. Typhimurium*, an organism we found in previous work to have higher intrinsic resistance to PUDs and PU films.²¹ Specifically, the two most active PU films from the disk diffusion work, along with the negative control polymer A1-

anionic (abbreviated hereafter as “A1-AN”), were examined for their potential to leach antibacterial components into liquid media. We also sought to examine the impact of PU films on the physical integrity and viability of *S. Typhimurium* suspensions. These experiments are described in greater detail below.

Leaching of antibacterial components from dried films. To determine whether or not substantial leaching of antibacterial material from cast films could occur, the following experiment was performed. Two hundred microliters of each test PUD (A1-AN, B2 and B3) were added to separate 8 mL sterile screwcap tubes and allowed to air dry in a sterile biological safety cabinet for 2 days, yielding tubes containing dried films at the bottom. The abilities of these films to affect the growth of *S. Typhimurium* in media added to these tubes was examined visually using a resazurin-based test. Briefly, 3 mL of TSB inoculated with *S. Typhimurium* (10^5 CFU mL⁻¹) was added to tubes containing each film type. As a positive control, the same amount of cell culture was also added to an unmodified sterile tube (no PUD film). An uninoculated tube of sterile TSB served as a negative control. After incubation at 35 °C for 20 hours, the oxidation-reduction indicator resazurin (alamarBlue®, Trek Diagnostic Systems, Cleveland, OH) was added into each tube to visually test the inhibitory effects of leaching components from PU films.²⁶ Briefly, when live, metabolically active cells were present, the dye underwent a color change from blue to pink. In media to which no cells were added or where cell viability was reduced or eliminated, the dye remained blue.

As another means for examining the degree of leaching of active PU film components into liquids, we exposed sterile bacterial growth media to the three types of PU films, then examined the subsequent ability of each medium to support growth of *S. Typhimurium*.

Briefly, 3 mL of sterile TSB was added to tubes containing each type of film, prepared as described above. As a control, the same volume of TSB was added to an unmodified sterile tube (no PUD film). All tubes were incubated for 3 days at 35 °C, allowing any diffusible components of the film to partition into the TSB medium. PUD-exposed and control media were collected and dispensed into individual wells of a Bioscreen C Microbiological Reader plate (Growth Curves, USA, Piscawatay, NJ). Wells were inoculated with *S. Typhimurium* (10^5 CFU mL⁻¹) and the plates were incubated for 24 h at 35 °C in the Bioscreen, with absorbance readings taken every 15 min at 600 nm. To examine the potential impact of heat exposure on the nutrient content of TSB during the 3 day leaching period, fresh TSB was also tested in parallel with the other treatments.

Assay for intracellular leakage from PUD-exposed Salmonella. The impact of PUD exposure on the physical integrity of *S. Typhimurium* was examined using a spectrophotometric assay for leakage of intracellular components. Briefly, an overnight culture of *S. Typhimurium* was harvested and cells were suspended in 0.85% saline at a concentration of 10^9 CFU mL⁻¹. One milliliter aliquots of this suspension were added to screwcap tubes coated with A1-AN, B2 or B3 PUD films or, as a control for the effects of saline alone, to an unmodified sterile tube (no PUD film). These were incubated for up to 24 h at 35 °C. After 1, 3, 5, 7 or 24 hours exposure, 100 µL portions were removed for analysis. These were diluted in 200 µL 0.85% saline and centrifuged for 6 min at 16,600 x g to ensure that the supernatant contained only macromolecular material released during PU film exposure. Two hundred microliters of this clarified supernatant were removed to a new centrifuge tube and the absorbance read at 260 nm using a BioMate 3 spectrophotometer (Thermo Fisher Scientific, Waltham, MA).²⁷ Appropriate blanks were used to control for

any potential contribution of PUD material to UV absorbance. Viability testing was also carried out in parallel at each timepoint. Briefly, PUD-containing tubes were vortexed to suspend cells and aliquots were taken, serially diluted into 0.85% saline and viable cells quantified using the track dilution method.²⁸ The relationship between the rate of leakage of UV-absorbing intracellular material and the death rate for *S. Typhimurium* was plotted using the combined spectrophotometric and plate count data from the 3 h, 5 h and 7 h timepoints, during which OD increased in a linear fashion. Briefly, the slope for each OD curve over this initial 4 h period was calculated for the three PU films, and these data were plotted against the death rate (\log_{10} reduction hr^{-1}).²⁹ This plot provides another means for ordering the PU films in terms of their efficacy against *S. Typhimurium*.

Results and Discussion

Thermal and Mechanical Properties. Dynamic mechanical analysis (DMA) was used to elucidate the thermal and mechanical properties of the PU films. The results are summarized in Tables 2 and 3. As the relative molar ratio of MDEA increases, the T_g increases from 14.3 to 20.0 °C (see Table 2). Likewise, the storage modulus at room temperature (25 °C) increased from 126.1 to 406.8 MPa. The PU films with higher amounts of MDEA, a chain extender, have improved mechanical properties because the increases also correspond to increases in overall hard segment content supplied by the IPDI.¹⁴ Likewise, increasing the hydroxyl numbers of the soy polyol while keeping the overall molar ratios between NCO and OH constant, raises the crosslink density of the PU films.¹⁴ This is demonstrated by the increase in the T_g from 3.0 to 17.8 °C as the hydroxyl number changes from 140 to 174 mg KOH/g (see Table 3). The storage modulus at 25 °C increased from 21.0 to 211.6 MPa. The trends from increasing MSOL hydroxyl number and from increasing MDEA and IPDI molar

ratios are illustrated together for the storage modulus in Figure 1 and for the glass transition temperature in Figure 2. Additionally, as a reference, one anionic PU film with DMPA instead of MDEA was evaluated. The anionic PU had a much higher T_g (20.6 vs 3.0 °C) and storage modulus at 25 °C (305.3 vs 21.0 MPa) compared to the cationic PU sample with the same IPDI molar ratios due to the physical differences between DMPA and MDEA. Differential scanning calorimetry (DSC) was also used to examine the thermal properties of the PU films (data not shown). The thermograms for the films showed single, but broad glass transition temperatures that are consistent with amorphous (non-crystalline) polymers.

Table 2. Comparison of DMA and TGA data of PU films with different ratios of MDEA.

Sample	OH Ratio from MDEA	wt% MDEA	T_g (°C) ^a	E' at 25 °C (MPa)	TGA Data		
					T_5 (°C)	T_{50} (°C)	T_{max} (°C)
B1	0.95	8.83	14.3	126.1	248.2	360.4	350.1
B2	1.45	11.95	16.7	219.5	195.5	348.9	346.3
B3	1.70	13.18	20.0	406.8	192.9	347.8	349.0

^a T_g based on onset of storage modulus

Table 3. Comparison of DMA and TGA data of PU films with different hydroxyl numbers.

Sample	OH Number	wt% MDEA	T_g (°C) ^a	E' at 25 °C (MPa)	TGA DATA		
					T_5 (°C)	T_{50} (°C)	T_{max} (°C)
A1-AN ^b	140	--	20.6	305.3	170.4	351.7	384.5
A1	140	8.32	3.0	21.0	246.3	355.3	342.2
B1	155	8.83	14.3	126.1	248.2	360.4	350.1
C1	174	9.41	17.8	211.6	215.6	306.3	284.6

^a T_g based on onset of storage modulus

^b A1-AN. This PUD has the same structural backbone as PUD A1, but is anionic. A1-AN serves here as a negative control, confirming that a cationic charge is required for antibacterial activity.

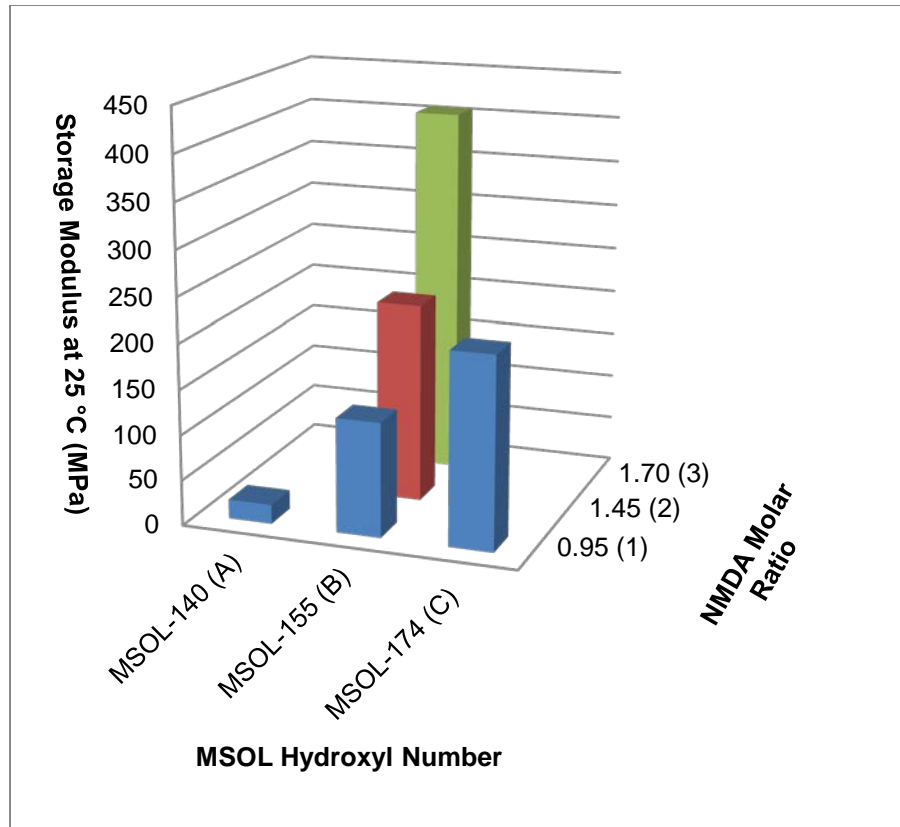


Figure 1. Storage modulus at 25 °C for PU films with different compositions.

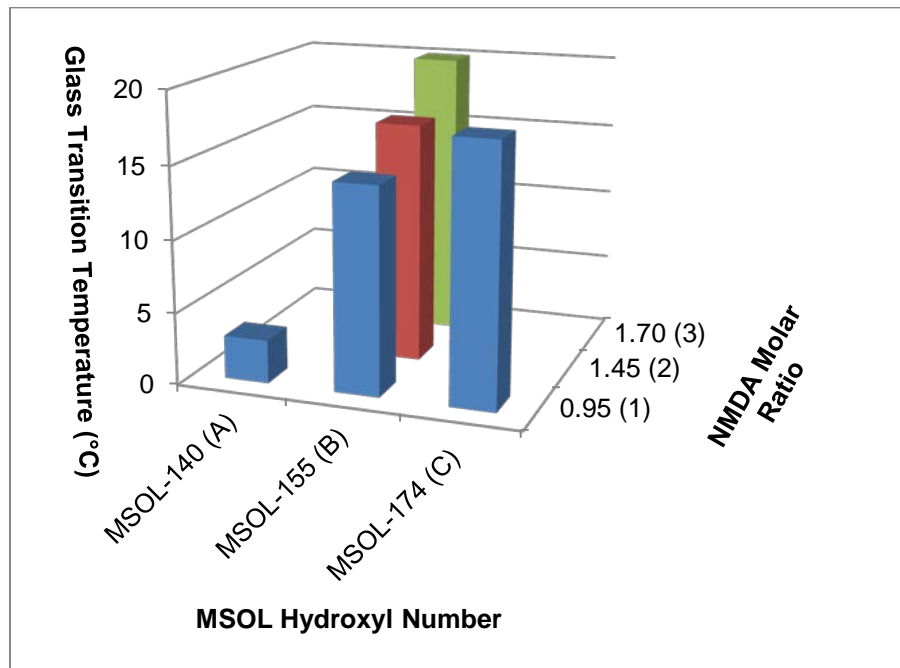


Figure 2. Glass transition temperatures for PU films with different compositions

Figure 3 displays the weight-loss and derivative weight-loss curves as a function of temperature for PU films with different ratios of MDEA. The increase in both IPDI and MDEA increases the amount of thermally labile ammonium and urethane groups. The samples with the highest relative ratios of ammonium groups had more pronounced derivative peaks for ammonium decomposition (below 200 °C) and dissociation of urethane bonds (200 to 320 °C). Figure 4 displays the weight-loss and derivative weight-loss curves as a function of temperature for PU films with different hydroxyl numbers. Although higher OH number results in higher crosslinking, as reflected by increases in the T_g , the higher OH number incorporates more IPDI, resulting in more urethane groups, thereby decreasing the thermal stability.

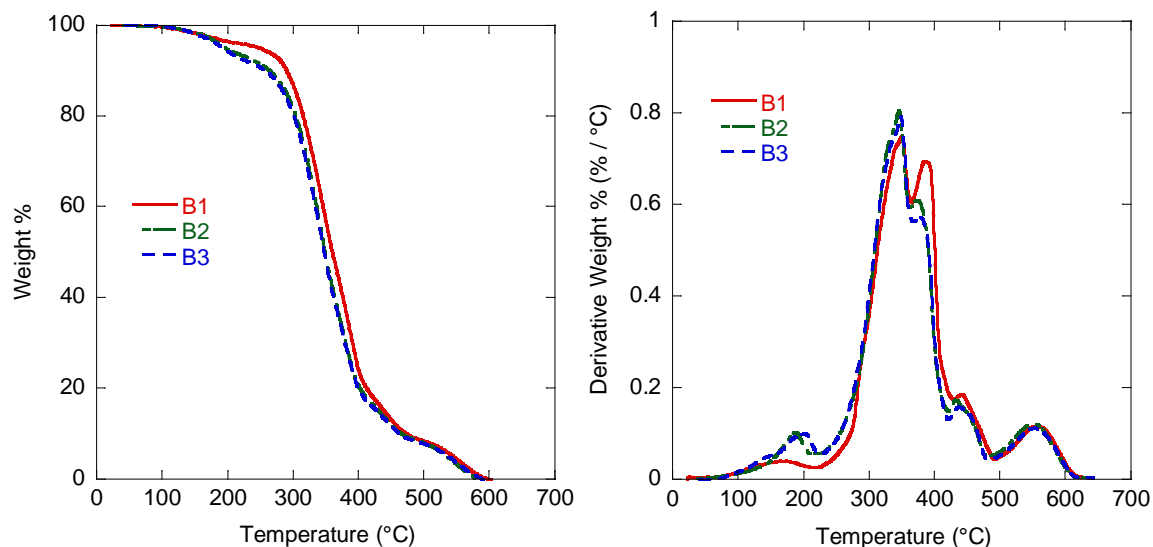


Figure 3. Thermogravimetric analysis (TGA) curves and their derivative curves for PU films with different molar ratios of MDEA

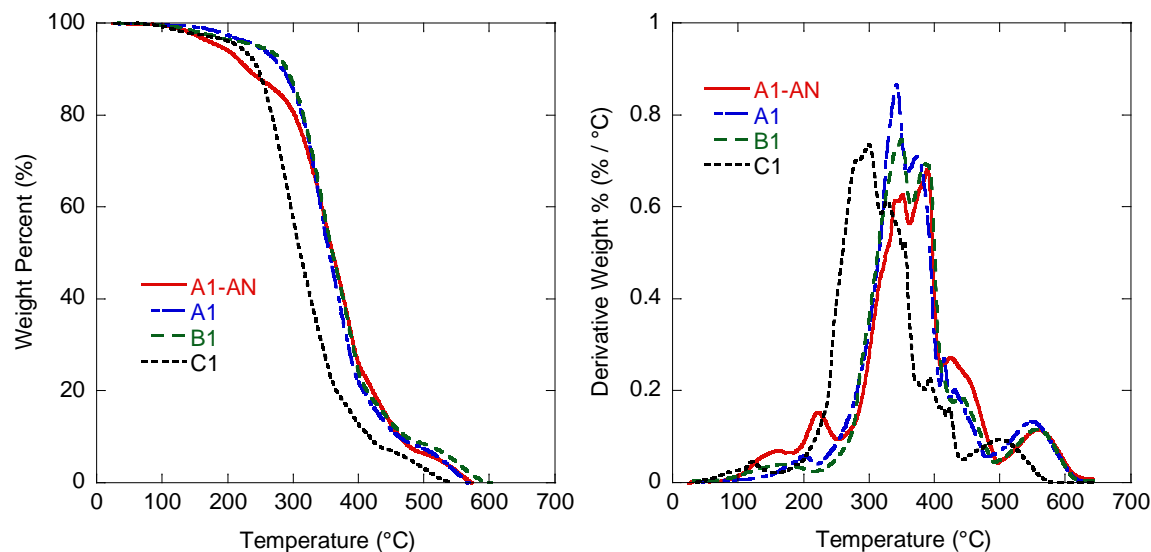


Figure 4. Thermogravimetric analysis (TGA) curves and their derivative curves for PU films with different hydroxyl numbers.

Antibacterial Properties. Based on the results of disk diffusion tests for PU dispersions and films, as the MDEA OH molar ratio increased from 0.95 to 1.45 (samples B1 to B2), zones of inhibition also increased significantly (see Table 4). These results indicate that antibacterial properties increase as the relative concentration of quaternary ammonium groups in the polymer backbone increases (from 8.8 wt% to 12.0 wt% MDEA for B2 and B3, respectively). However, there was no significant difference between B2 (MDEA OH molar ratio of 1.45) and B3 (MDEA molar ratio of 1.7) in this assay. This can be attributed to the smaller change in the concentration of quaternary ammonium groups from B2 to B3 (12 wt% MDEA to 13.2 wt% MDEA).

Table 4. Summary of disk diffusion testing

	<i>L. monocytogenes</i> NADC 2045		<i>S. Typhimurium</i> ATCC 13311		<i>S. aureus</i> ATCC BAA-44	
	ZOI ^a (diameter in mm)		ZOI ^a (diameter in mm)		ZOI ^a (diameter in mm)	
	Dispersion	Film	Dispersion	Film	Dispersion	Film
A1-AN ^b	None	None	None	None	None	None
A1	11.65 ± 0.22	11.12 ± 0.12	9.75 ± 0.16	9.04 ± 0.21	9.74 ± 0.16	9.28 ± 0.16
B1	10.79 ± 0.17	10.48 ± 0.27	9.15 ± 0.17	8.18 ± 0.23	9.18 ± 0.12	8.35 ± 0.13
B2	11.94 ± 0.15	11.43 ± 0.13	10.48 ± 0.22	9.57 ± 0.21	10.68 ± 0.16	10.23 ± 0.28
B3	11.92 ± 0.32	11.33 ± 0.17	10.29 ± 0.12	9.56 ± 0.29	10.74 ± 0.18	10.00 ± 0.06
C1	10.93 ± 0.27	10.23 ± 0.19	9.11 ± 0.11	8.02 ± 0.16	9.63 ± 0.13	8.56 ± 0.11

^a ZOI: Zone of Inhibition

^b A1-AN. This PUD has the same structural backbone as PUD A1, but is anionic. A1-AN serves here as a negative control, confirming that a cationic charge is required for antibacterial activity.

The polyurethanes made with polyols with larger hydroxyl values have an increased crosslink density as a result of the higher hydroxyl functionality. By changing the hydroxyl functionality while keeping the molar ratios of MDEA constant, samples prepared from polyols with larger hydroxyl values have slightly higher quaternary ammonium concentrations. However, PU sample A1, which had the lowest hydroxyl number (140 mg KOH/g) and the lowest quaternary ammonium concentration (8.3 wt% MDEA), showed better antibacterial properties than the corresponding samples B1 and C1 with higher hydroxyl numbers and higher quaternary ammonium concentrations. This trend indicates that the polymers with lower crosslink densities have better antimicrobial properties. The higher molecular mobility of these less crosslinked polymers likely enhances effective physical interaction with target bacteria, resulting in a net increase in antibacterial activity.

The same relative trend of antibacterial activity was observed for all three strains tested in our disk diffusion assay. *L. monocytogenes* was most susceptible to the PUDs and

PU films tested, and *S. Typhimurium* was the least susceptible ($p < 0.05$). The greater resistance of *Salmonella* to PUD activity can be explained by the outer membrane (OM) of this Gram-negative bacterium, which serves as an additional permeability barrier to exogenous compounds. The absence of an OM in Gram-positive bacteria such as *L. monocytogenes* and *S. aureus* allows more ready uptake of antimicrobials by these bacteria and is consistent with earlier findings by Xia et al.²¹

By their very nature, the disk diffusion tests indicated that dried films were capable of releasing diffusible antibacterial material into the agar medium. In practical use, the mobility of material from films could be problematic for food-related applications, where chemical residues are not desirable. Therefore, we sought to examine the potential importance of leaching from cast films in more detail. In these tests, the most active PUs (B2 and B3) were examined further against *S. Typhimurium* in liquid systems using both qualitative and quantitative assays. Figure 5 shows that PU film B3 could effectively inhibit the growth of this pathogen inoculated at 10^5 CFU ml⁻¹ into TSB. Although PU B2 did not prevent growth of *S. Typhimurium* under these conditions, it did possess good antibacterial activity, as determined by the disk diffusion and cell leakage assays. This underlines the importance of using multiple types of analyses when evaluating and ranking antimicrobial activity. The negatively-charged A1-AN did not show antibacterial activity, as expected given the known relationship between cationic charge and antimicrobial efficacy. While the results of this assay suggest that diffusible polymer elements could be responsible for the growth inhibition seen, it is also possible that inactivation of cells could have resulted through direct contact with the film at the bottom of the tubes. The test for leaching (Figure 6) shows that antibacterial components were able to diffuse from films into TSB held for 3 days at 35°C

and exert their activities in solution. This assay also provides clear corroboration that A1-AN is not inhibitory, and that both B2 and B3 are antibacterial, with B3 being the most active. The greater activity of B3 indicates that the molar ratio of MDEA had an impact on antibacterial activity.

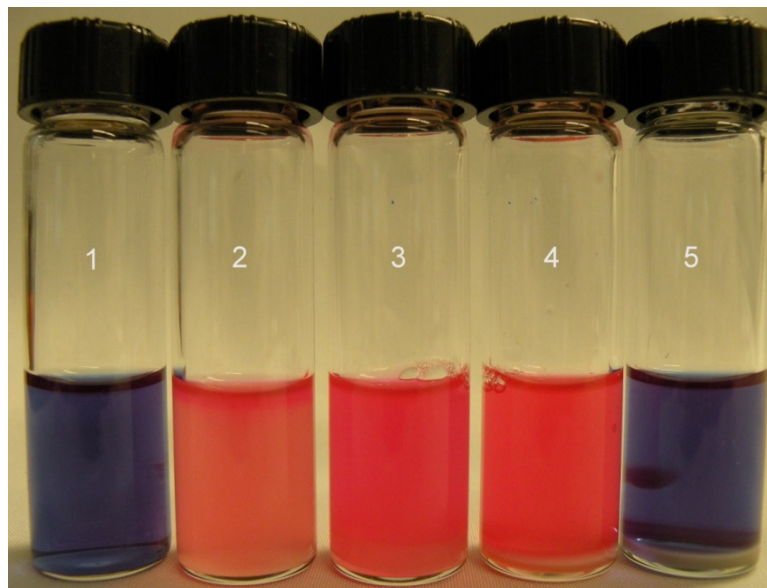


Figure 5. Visual demonstration of bacterial inhibition in tubes containing PU films. The following treatments were examined: 1. negative control (uninoculated TSB, no PU coatings), 2. Positive control (no PU coatings), 3. A1-AN coating (negative control), 4. B2 coating, 5. B3 coating. Treatments 2-5 were inoculated with *S. Typhimurium* ATCC 13311 at 10^5 CFU mL⁻¹.

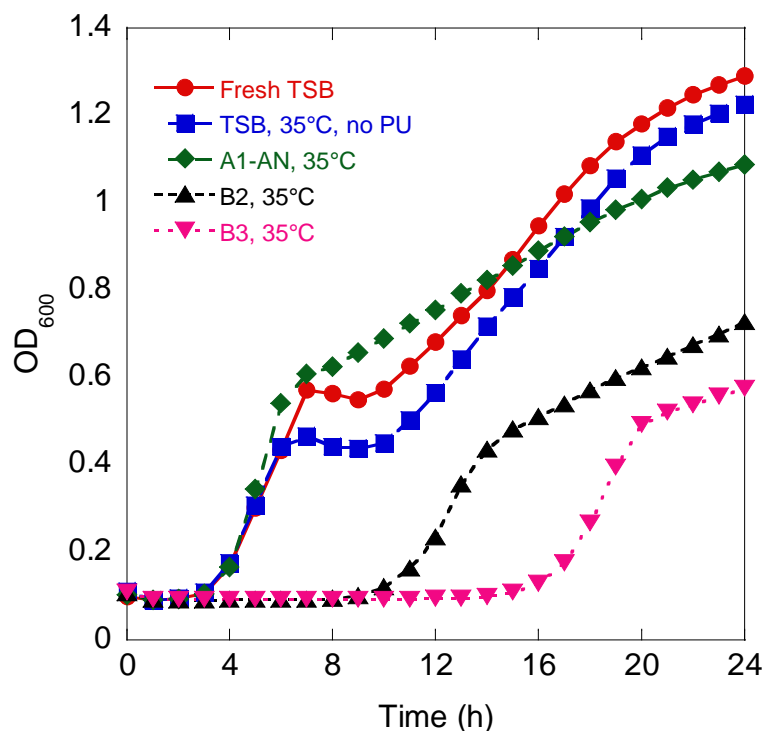


Figure 6. Results of antibacterial leaching assay. Effects of the following treatments on growth of *S. Typhimurium* ATCC 13311 in TSB were examined in a Bioscreen C automated turbidimeter: fresh, untreated TSB; TSB pre-incubated for 3 days at 35°C; and TSB incubated for 3 days at 35°C in the presence of the films A1-AN, B2 and B3, respectively. Absorbance was measured at 600 nm. Decreased absorbance indicates suppression of bacterial growth.

Based on the known action of other cationic antimicrobials, we expected that the PUDs and their films might exert their antibacterial activities by causing gross physiological damage to bacterial cells. We tested this hypothesis by assaying for leakage of UV-absorbent materials (i.e. DNA, proteins, other macromolecules) from bacterial cells and into the surrounding medium. Our results from the intracellular leakage assay agreed with those of the film leaching assay, with A1-AN yielding little more damage to cells than did exposure to saline alone, and polymers B2 and B3 causing a steady increase in loss of intracellular contents to the medium (Figure 7a). These results confirm that antibacterial components capable of permeabilizing this Gram-negative bacterial pathogen are able to leach into liquids

from these PU films. Figure 7b shows that over the 24 h period, exposure to B2 and B3 films resulted in a ~4-log reduction in viable cells. Conversely, exposure to the A1-AN film, as with saline alone, did not cause cell death. These results mirror those of the UV leakage assay, demonstrating that increasing exposure of *S. Typhimurium* cells to diffusible elements from the cationic PU films results in increased permeability, loss of cellular contents and cell death. The relationship between the rate of leakage of UV-absorbent material and the cell death rate over the period extending from 3 h to 7 h exposure is plotted in Figure 7c. This plot demonstrates that B3 was the most effective antibacterial film, followed by B2, and finally by A1-AN, which was not antibacterial.

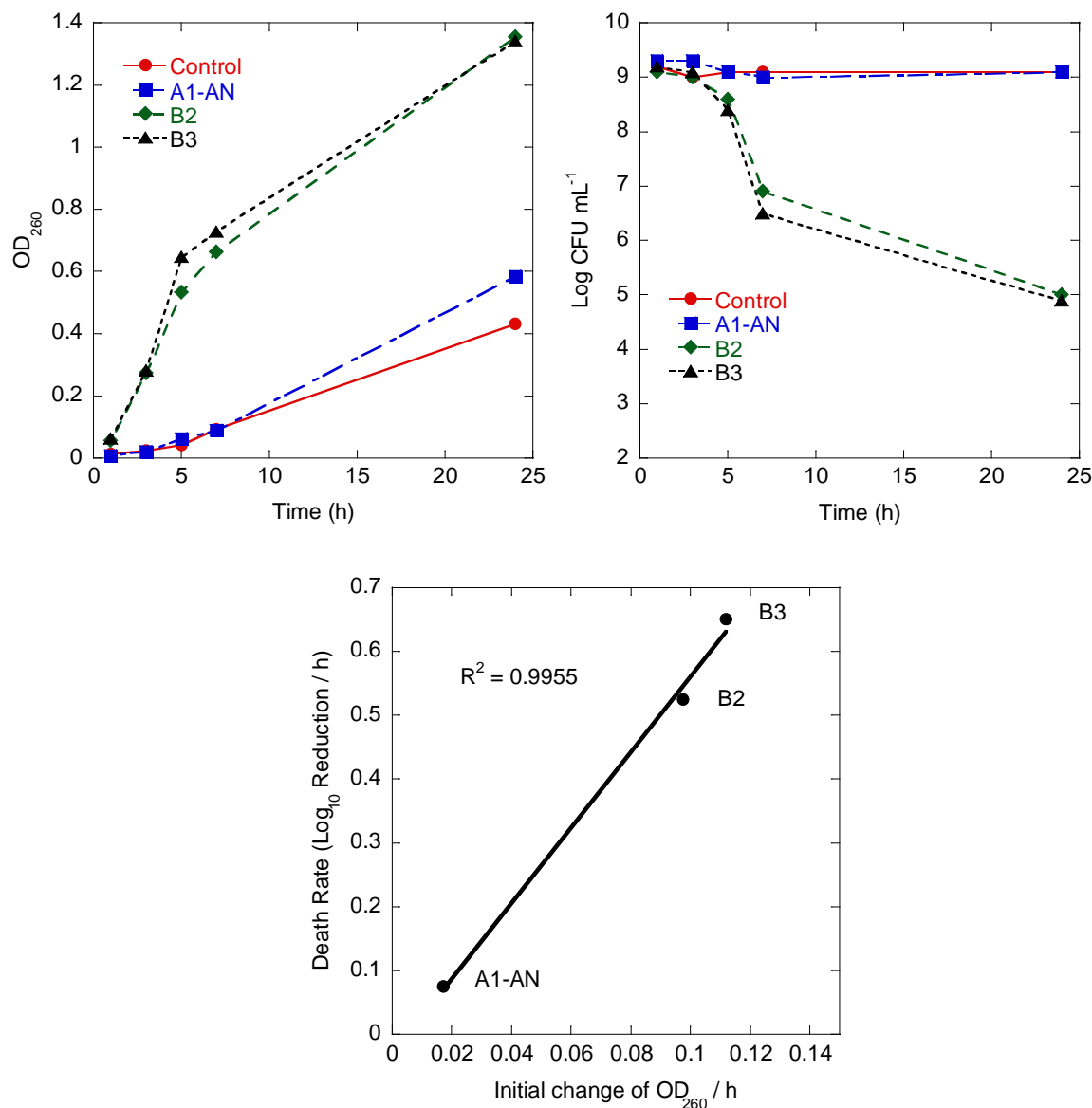


Figure 7. PU film-mediated leakage of intracellular components from *S. Typhimurium* ATCC 13311. Cells were suspended in 0.85% saline at 10^9 CFU mL⁻¹ and exposed to tubes coated with films A1-AN, B2 or B3 as described in Materials and Methods. Leakage of UV-absorbing intracellular components was followed over a 24 h period at 260 nm. Increases in UV-absorbance indicated physical permeabilization of cells and leakage of cellular macromolecules.

- Absorbance vs. time for cell suspensions exposed to saline alone (control) or tubes containing PU films A1-AN, B2 or B3.
- Viability vs. time for cell suspensions analyzed in Fig 7a. PU film-exposed cell suspensions were plated in parallel with absorbance readings.
- Relationship between rate of leakage at 260 nm and death rate for *S. Typhimurium* ATCC 13311 exposed to PU films A1-AN, B2 or B3. Data were plotted from the initial period of linear OD increase extending from hours 3 to 7.

Conclusions

Soybean-oil based cationic PUDs have been prepared with three different relative compositions of ammonium cations. Additionally, cationic PUDs were prepared using soy polyols with three different hydroxyl numbers. The glass transition temperatures and room-temperature storage moduli both increased with the increase in MDEA and IPDI molar ratios, as well as with increases in the hydroxyl number of the soy polyol. All of the cationic PUDs were found to have inhibitory activity against three foodborne pathogens, *Salmonella* Typhimurium, *Listeria monocytogenes*, and methicillin-resistant *Staphylococcus aureus*. Increasing the relative ratio of ammonium cations improved the antibacterial properties, however the results show that this effect may level out around 12 wt% MDEA. This observed trend was consistent across the different bacterial strains. This investigation shows promising results in that the mechanical properties of environmentally-friendly, soy-based cationic PUDs can be tuned while maintaining their antibacterial activity. Antibacterial components were able to diffuse from these films into liquid media, exerting their activities in solution. These components caused death of *S. Typhimurium* through disruption of the barrier structures responsible for keeping cellular macromolecules inside and exogenous molecules outside (the outer membrane and cell membrane, for example). These PUDs and PU films were active against *L. monocytogenes* and *S. Typhimurium*, the two leading bacterial causes of foodborne disease outbreaks, and against methicillin-resistant *S. aureus*, an important clinical pathogen with emerging relevance to food safety. Together, our results indicate that these PUDs and PU films are effective antibacterial materials with mechanical and physical properties that can be tailored to meet the needs of specific applications. Because we demonstrated diffusive loss of antibacterial material from PU films, additional

work is required to determine the suitability of these materials for applications involving direct contact with foods. However, additional non-contact uses are possible, such as coating of shipping pallets used in food storage or shipping operations, which have been implicated as points of harborage for human pathogens.

Acknowledgments

We gratefully acknowledge financial support from the Consortium for Plant Biotechnology Research (CPBR) and the Archer Daniels Midland (ADM) Company.

References

1. M. Desroches, M. Escouvois, R. Auvergne, S. Caillol and B. Boutevin, *Polym. Rev.*, 2012, **52**, 38.
2. M. A. R. Meier, J. O. Metzger and U. S. Schubert, *Chem. Soc. Rev.*, 2007, **36**, 1788.
3. A. Gandini, *Macromolecules*, 2008, **41**, 9491.
4. Y. Xia and R. C. Larock, *Green Chem.*, 2010, **12**, 1893.
5. R. P. Wool and S. N. Khot, *ASM International*, 2001, 184.
6. Z. S. Petrovic, *Polym. Rev.*, 2008, **48**, 109.
7. J. K. Fink, *Reactive Polymer Fundamentals and Applications: A Concise Guide to Industrial Polymers*, William Andrew Publishing, Norwich, NY, 2005.
8. H. Fu, H. Huang, Q. Wang, H. Zhang and H. C. HQ, *J. Disper. Sci. Technol.*, 2009, **30**, 634.
9. V. García-Pacios, V. Costa, M. Colera and J. M. Martín-Martínez, *Prog. Org. Coat.*, 2011, **71**, 136.
10. V. García-Pacios, V. Costa, M. Colera and J. Miguel Martín-Martínez, *Int. J. Adhes. Adhes.*, 2010, **30**, 456.
11. B. K. Kim, *Colloid Polym. Sci.*, 1996, **274**, 599.
12. B. K. Kim and J. C. Lee, *J. Polym. Sci. Pol. Chem.*, 1996, **34**, 1095.
13. A. Patel, C. Patel, M. G. Patel, M. Patel and A. Dighe, *Prog. Org. Coat.*, 2010, **67**, 255.
14. Y. Lu and R. C. Larock, *Biomacromolecules*, 2008, **9**, 3332.
15. V. D. Athawale and R. V. Nimbalkar, *J. Disper. Sci. Technol.*, 2011, **32**, 1014.
16. Y. Lu and R. C. Larock, *ChemSusChem*, 2010, **3**, 329.
17. Y. Lu and R. C. Larock, *Prog. Org. Coat.*, 2010, **69**, 31.
18. S. Sundar, N. Vijayalakshmi, S. Gupta, R. Rajaram and G. Radhakrishnan, *Prog. Org. Coat.*, 2006, **56**, 178.
19. C. Campos, L. N. Gerschenson and S. Flores, *Food Bioprocess Tech.*, 2011, **4**, 849.
20. M. Cécius and C. Jérôme, *Prog. Org. Coat.*, 2011, **70**, 220.
21. Y. Xia, Z. Zhang, M. R. Kessler, B. Brehm-Stecher and R. C. Larock, *ChemSusChem*, 2012, **5**, 2221.

22. E. Scallan, R. M. Hoekstra, F. J. Angulo, R. V. Tauxe, M. A. Widdowson, S. L. Roy, J. L. Jones and P. M. Griffin, *Emerg. Infect. Dis.*, 2011, **17**, 7.
23. W. Zhang, J.-X. Zheng and G.-Y. Xu, *J. Food Sci.*, 2011, **76**, R76.
24. T. F. Jones, M. E. Kellum, S. S. Porter, M. Bell and W. Schaffner, *Emerg. Infect. Dis.*, 2002, **8**, 82.
25. A. M. O'Brien, B. M. Hanson, S. A. Farina, J. Y. Wu, J. E. Simmering, S. E. Wardyn, B. M. Forshey, M. E. Kulick, D. B. Wallinga and T. C. Smith, *PLoS One*, 2012, **7**.
26. R. K. Pettit, C. A. Weber, M. J. Kean, H. Hoffmann, G. R. Pettit, R. Tan, K. S. Franks and M. L. Horton, *Antimicrob. Agents Chemother.*, 2005, **49**, 2612.
27. R. Virto, P. Manas, I. Alvarez, S. Condon and J. Raso, *Appl. Environ. Microbiol.*, 2005, **71**, 5022.
28. B. D. Jett, K. L. Hatter, M. M. Huycke and M. S. Gilmore, *Biotechniques*, 1997, **23**, 648.
29. A. F. Mendonca, T. L. Amoroso and S. J. Knabel, *Appl. Environ. Microbiol.*, 1994, **60**, 4009.

CHAPTER 4. EFFECTS OF COUNTERIONS ON THE PHYSICAL AND ANTIMICROBIAL PROPERTIES OF CASTOR OIL-BASED CATIONIC POLYURETHANE COATINGS

Introduction

Aqueous polyurethane dispersions (PUDs) are highly useful coating materials that have found widespread applications in coatings, adhesives, paper sizings, and textiles.^{1,2} The resulting polyurethane films are known for their toughness, tensile strength, abrasion resistance, and excellent film forming properties.^{3,4} Furthermore, waterborne coatings, including polyurethane dispersions, have significant advantages over conventional solvent-borne coatings as a result of regulations restricting the emissions of volatile organic compounds from organic solvents.^{3,5,6}

Conventional polyurethanes are hydrophobic and require either the use of external emulsifiers or large shear forces to disperse in water.^{3,7} However, polyurethanes can be readily dispersed or dissolved in water by incorporating hydrophilic copolymers, called ionomers, into the polyurethane chains. Ionomers contain functional groups, such as acids or tertiary nitrogen groups, that can be neutralized or quaternized, respectively, to form salts.⁸ The extent of neutralization or quaternation, which can range from partial to complete neutralization, has been shown to impact the stability and particle size of the PUDs.^{9,10} A higher degree of neutralization has been found to increase the tensile strength, modulus and glass transition temperature due to increased interchain interactions and hydrogen bonding.¹¹ Ionomers can be classified by the charges incorporated in the main polymer chain: anionomers (negatively charged), cationomers (positively charged), and zwitterionomers (both positive and negatively charged).^{3,7,12} The majority of commercial PUDs use anionic

ionomers.^{7,13} In particular, dimethylolpropanoic acid (DMPA) has been one of the most widely used anionomers for PUDs.^{10,13}

Anionic PUDs have been extensively studied, including a number of investigations focused on the role of the counterion.¹⁴ The studies have shown that the counterion does influence the thermal and mechanical properties of the polyurethane films, particularly the thermal stabilities.¹⁴ A variety of bases have been used as counterions in anionic PUDs, including amines and metal hydroxides.^{15,16} Increased ionization of the carboxylic acid groups has been shown to decrease the onset temperature of decomposition in anionic PUDs.¹⁶ Neutralization of anionomers with metal hydroxides has yielded films with increased initial thermal stabilities due to the involatility of the metal carboxylate products.^{14,16,17} Degradation of thermally labile ionomers, such as phosphate groups, has been shown to be dependent on the neutralizing base.^{14,17} Increases in the ionic potential of counterions has corresponded to increased tensile strength, decreased elongation at break, and decreased particle size when anionic PUDs were neutralized with different metal hydroxides and amines.¹⁵ The glass transition temperature has also been shown to be impacted by counterions.^{12,18}

More recently, cationic PUDs are gaining attention because of the antimicrobial activity of quaternary amines.¹⁹⁻²¹ In particular, antimicrobial cationic polyurethane coatings are well suited for paper coating applications since cationic polymers strongly adhere to fiber surfaces.²² Cationic PUDs are typically synthesized by reacting diisocyanates with nitrogen-containing alkyl diols, such as *N*-methyldiethanolamine (MDEA).^{14,23,24} The nitrogen atoms are subsequently quaternized, either by protonation with acids or by an S_N2 reaction with alkyl halides, to produce the ionic groups.^{19,24,25} Previously, our group has examined the

effect of different amino polyols on the thermal, mechanical, and antimicrobial properties of vegetable oil-based cationic PUDs.²⁰ Our group has also investigated the effects of MDEA molar ratios and different hydroxyl numbers of soybean oil-based polyols on vegetable oil-based cationic PUDs.²⁶

In the current study, the effect of the counteranion on the thermal, mechanical, and antimicrobial properties of cationic castor oil-based PUDs and their films has been evaluated for the first time. Previous studies on the effect of counterions have been largely limited to counteranions of anionic ionomers. The cationic castor oil-based PUDs have been prepared from seven different carboxylic acids: formic acid, acetic acid, propanoic acid, butanoic acid, isobutyric acid, acrylic acid, and lactic acid. In this study, the effect of carboxylic acid chain length has been examined as the carboxylic acids range in size from one to four carbons (formic acid < acetic acid < propanoic acid < butanoic acid). Furthermore, the effect of substituents (hydrogen, hydroxyl, or methyl group) and unsaturation has been examined as shown in Figure 1. The biorenewable castor oil-based coatings reported in this study appear promising for applications requiring antimicrobial functionalized surfaces.

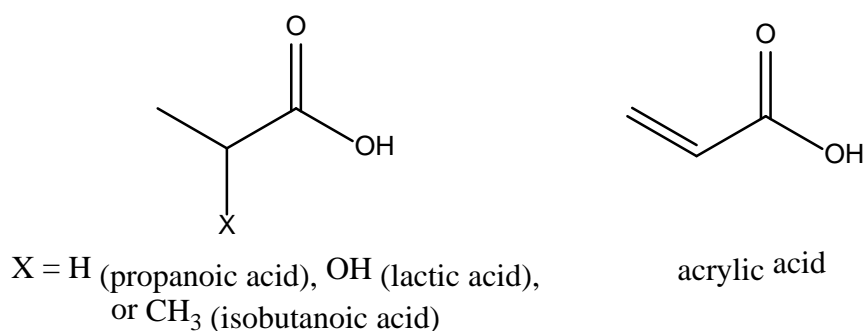
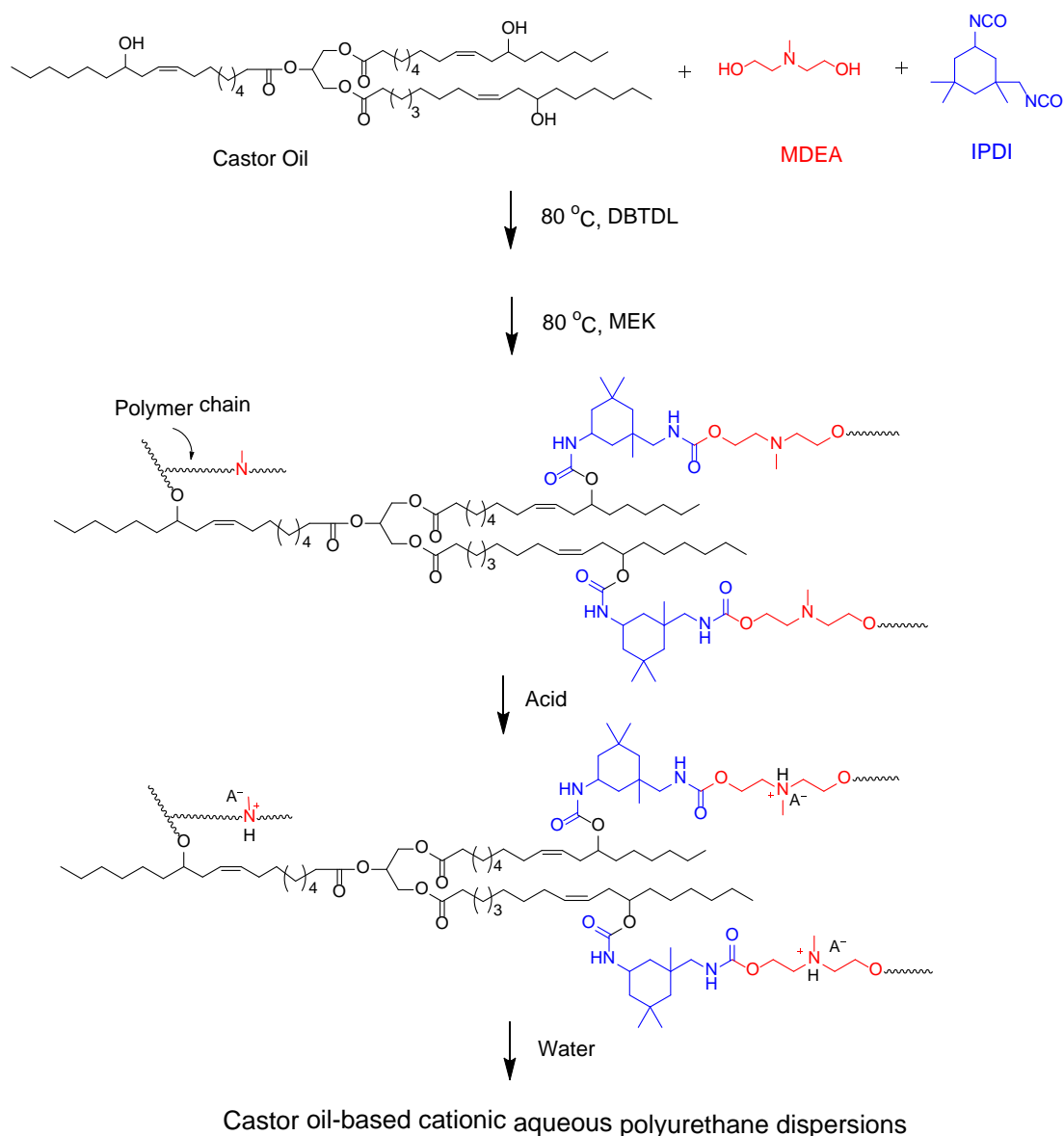


Figure 1. Structure of various carboxylic acids used to neutralize the amino groups

Experimental

Materials. Castor oil, *N*-methyl diethanolamine (MDEA), isophorone diisocyanate (IPDI), dibutyltin dilaurate (DBTDL), acrylic acid, butanoic acid, isobutyric acid, and lactic acid were purchased from Sigma-Aldrich (Milwaukee, WI, USA). Methyl ethyl ketone (MEK), acetic acid, formic acid, and propanoic acid were purchased from Fisher Scientific Company (Fair Lawn, NJ, USA). All materials were used as received.

Synthesis of the Castor Oil-based Cationic PUDs. The synthesis of the castor oil-based cationic PUDs was carried out using different organic acids (formic, acetic, propanoic, butanoic, acrylic, lactic, and isobutyric acids) to neutralize the amino groups. The detailed experimental procedure shown in Scheme 1 follows. Castor oil (5.00 g), IPDI (4.43 g), MDEA (1.47 g), and one drop of DBTDL were added to a three-necked flask equipped with a mechanical stirrer, thermometer, and condenser. The molar ratio of the OH groups from the castor oil, the NCO groups from the IPDI, and the OH groups from the MDEA was kept as 1.0 : 2.75 : 1.7. The reaction was first carried out at 80 °C and, after approximately 10 min, MEK (25 mL) was added to reduce the viscosity. After 2 h of reaction, the reactants were then cooled to room temperature and neutralized by the addition of 2.0 equivalents of acid, followed by dispersing at high speed with distilled water to produce the cationic PUD with a solid content of about 13 wt% after removal of the MEK under vacuum. The corresponding PU films were obtained by drying the resulting dispersions at room temperature in a polytetrafluoroethylene mold. The nomenclature used for the resulting castor oil-based cationic PUDs is as follows: the PUD quaternized with butanoic acid was designated as PU-Butanoic.



Scheme 1. Preparation of the castor oil-based cationic aqueous polyurethane dispersions

Characterization. The weight loss of the PU films under an air atmosphere was measured by using a thermogravimeter (TA Instruments Q50). Samples (≈ 8 mg) were heated from room temperature to 650 °C at a heating rate of 20 °C/min. One representative PU film sample (PU-Butanoic) was analyzed by evolved gas analysis using a thermogravimeter coupled with a mass spectrometer (TA Instruments Q5000IR TGA interfaced to a Pfeiffer Thermostar mass spectrometer by means of a heated capillary transfer line). The sample was

kept isothermal at room temperature for 30 minutes and then heated from room temperature to 1000 °C at 20 °C/min. The capillary transfer line was heated to 195 °C. The Thermostar unit is based on a quadrupole design and the masses scanned ranged from 1-200 amu. The sample gas from the TGA was ionized at 70 eV. The purge gas was 25 mL/min nitrogen through the furnace and 10 mL/min nitrogen through the balance. The dynamic mechanical properties of the PU films were characterized by means of a dynamic mechanical analyzer (TA Instruments DMA Q800, New Castle, DE) using a film tension mode of 1 Hz in the temperature range from -60 to 100 °C with a heating rate of 5 °C / min. Rectangular samples with dimensions of 10 mm × 8 mm × 0.5 mm were used for the analysis. DSC analysis of the PU films was performed by means of a thermal analyzer (TA Instruments Q2000). PU samples (\approx 5 mg) were cut from the film and heated from room temperature to 100 °C to erase the thermal history. The samples were then equilibrated at -70 °C and heated to 150 °C at a heating rate of 20 °C/min. The T_g of PU films was determined from the midpoint in the heat-capacity change in the second DSC scan.

Results and Discussion

Thermogravimetric Analysis. The thermal degradation of polyurethanes is a complex process and thermal stability measurements are strongly dependent on the characterization methods.²⁷ Polyurethanes with different structures are known to exhibit different thermal stabilities.¹⁷ Previous research has reported three decomposition stages for vegetable oil-based cationic polyurethane dispersions: initial decomplexation of the ammonium groups, followed by decomposition of thermally labile urethane bonds, and then the decomposition of the fatty acids.²⁰ The initial decomposition of the ammonium groups primarily occurs below 200 °C, which was confirmed by thermogravimetric analysis combined with mass

spectrometric analysis (TG-MS) of the PU film neutralized with butanoic acid. In Figure 2a, the thermogravimetric spectrum shows the TGA data with a derivative weight peak at 165.9 °C ($t = 37.3$ min). The molecular ion peak of butanoic acid, $m/z = 88$, occurs in low abundance.²⁸ However, the base peak occurs at $m/z = 60$ for butanoic acid due, to the loss of an ethylene unit by McLafferty rearrangement.^{28, 29} In Figure 2b, the spectral data shows a strong overlap between a sharp peak for $m/z = 60$ and the first derivate weight peak, which confirms the decomposition of the amine complex below temperatures of 200 °C.

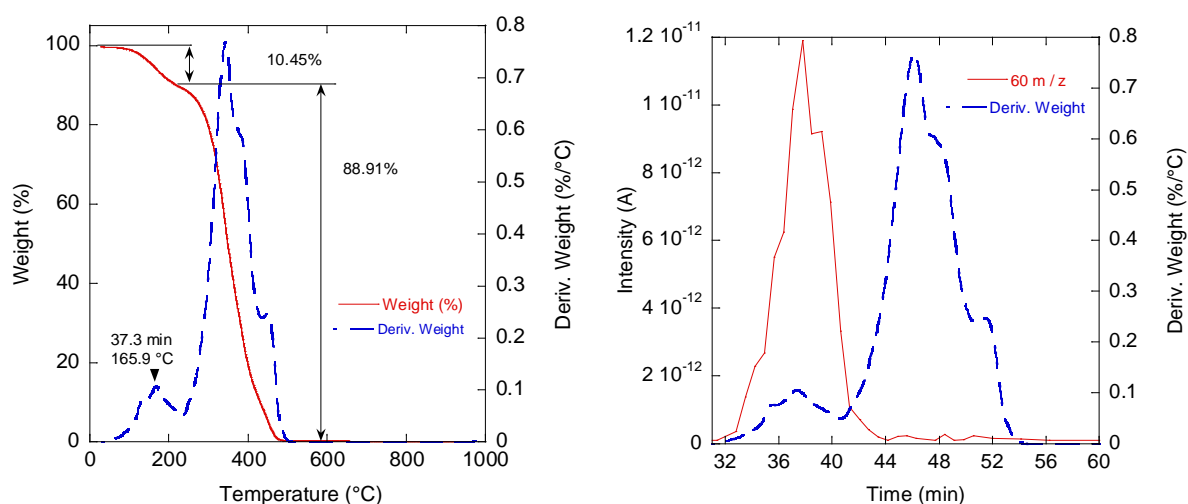


Figure 2. Thermogravimetric analysis with mass spectrometry (TG-MS) of a PU film neutralized with butanoic acid. a) Thermogravimetric analysis data. b) MS data and TGA weight derivative curve

TG-MS enables an estimation of the number of equivalents of acid remaining in the film. During the dispersion synthesis, 2 molar equivalents of acid per molar equivalent of amine groups were added to neutralize the amine groups. During film formation, the excess acid evaporated along with the water. However, we suspected that the larger carboxylic acids, *i.e.* butanoic acid or isobutyric acid, might remain trapped inside the film and act as a plasticizer. Furthermore, there were concerns that the excess residual amounts of acids could

interfere with the analysis of the antimicrobial activity. Organic acids are known to have antimicrobial activity against food-borne pathogens and are recognized as safe for people by the U.S Food and Drug Administration.³⁰ In order to address these concerns, TG-MS data has been used to estimate the wt% of excess butanoic acid retained by assuming all mass loss during the initial stage of decomposition is due to decomplexation of the acid molecules from the ammonium groups. The mass loss attributed to butanoic acid was 10.45 wt%, as shown in Figure 2. Theoretically, the minimum and maximum amounts of residual butanoic acid were 9.10 wt% and 16.7 wt%, respectively. Based on these amounts, we determined there were 1.15 equivalents of butanoic acid in the films, which corresponds to evaporation of 85% of the excess butanoic acid during film formation.

The thermograms of the polyurethane films neutralized with carboxylic acids of different chain lengths, shown in Figure 3, have decomposition profiles similar to the TG-MS thermogram of the PU-butanoic acid film. This is consistent with previous studies, which have reported the presence of oxygen does not significantly change the onset degradation temperature of ionomer polyurethanes compared to a nitrogen atmosphere.¹⁷

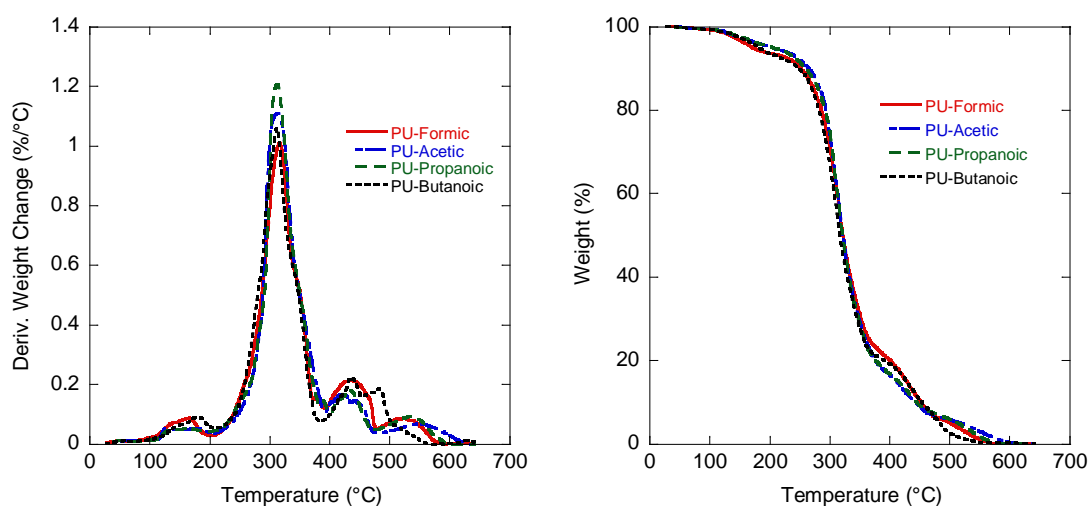


Figure 3. Thermograms of PU films neutralized with different chain length carboxylic acids

T_5 , T_{50} , and T_{max} for PU films neutralized with different chain length carboxylic acids are summarized in Table 1. T_5 , the temperature at which the samples lose 5 wt% of their mass, is a measure of the onset temperature of degradation.²⁰ No clear trend is observed in the T_5 results due to the large differences in molecular weight of the counteranions. After the initial stage of decomposition, the thermal stabilities of the different PU films are nearly identical. No significant difference is observed in the T_{50} and T_{max} values which is consistent with decomplexation of the ammonium groups prior to the urethane bonds breaking. Based on these results, as well as the TG-MS results for the PU-Butanoic film, we have used the TGA data to estimate the amount of residual acid in all of the PU films. For calculation purposes, decomposition of the amine complex was assumed to be complete prior to degradation of the urethane bonds. The base of the weight derivative corresponding to urethane was used as the reference point for the calculations. Increases in the molecular weight of the carboxylic acid correspond to increases in the wt% of acid in the PU films. The estimated wt% of acid and residual acid equivalents, listed in Table 1, show that the majority of the excess acid evaporated.

Table 1. Thermogravimetric results of PU films neutralized with different chain length carboxylic acids

PUD	T_5	T_{50}	T_{max}	wt% Acid	Residual Acid Equivalents
PU-Formic	170 ± 5	319 ± 2	312 ± 4	6.5 ± 0.5	1.2
PU-Acetic	206 ± 12	322 ± 1	315 ± 1	6.7 ± 0.5	1.1
PU-Propanoic	209 ± 6	320 ± 1	313 ± 1	8.2 ± 0.4	1.1
PU-Butanoic	180 ± 1	319 ± 4	312 ± 4	10.8 ± 0.5	1.2

Substituents on the carbon chain of the carboxylic acids have a more pronounced impact on the initial thermal stabilities and residual acid content of the PU films than the chain length of the carboxylic acid chains. The thermograms of the PU films with different substituents on the carboxylic acid carbon chains are shown in Figure 4 and the thermogravimetric data is summarized in Table 2. For this series of acids, the T_5 results can be used to compare onset temperatures since the range of molecular weights between propanoic acid, acrylic acid, isobutyric acid is smaller (74 g/mol for propanoic acid to 90 g/mol for lactic acid). The initial thermal stability and onset temperature of the PU-Lactic and PU-Acrylic films are significantly lower than those of the PU-Propanoic film. These observations are not explained by differences in molecular weight alone, as evidenced by the higher amounts of residual acid. For the PU-Lactic film, hydrogen bonding between the hydroxyl group on the lactic acid molecules and the polymer chain is a likely factor. Also, the sharp increase in the derivative weight peak around 100 °C indicates that the PU-Lactic film retained more water than other films. For the PU-Acrylic film, the carbon-carbon double bond makes acrylic acid more rigid than propanoic acid, which could explain the increased retention of acid in the corresponding PU film.

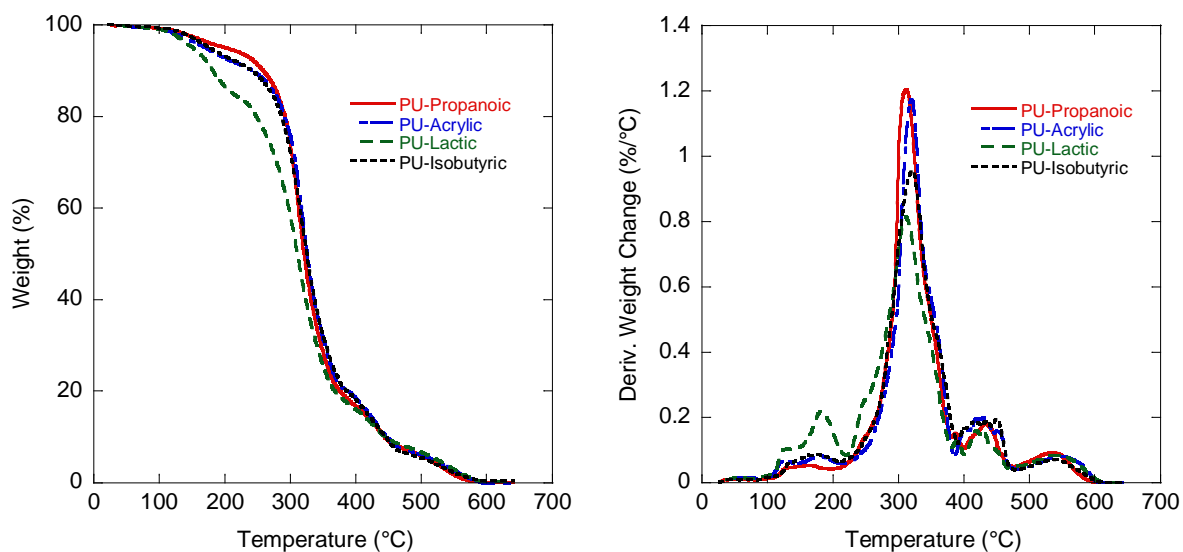


Figure 4. Thermograms of polyurethane films neutralized with carboxylic acids containing different substituents

Table 2. Thermograms of polyurethane films neutralized with carboxylic acids containing different substituents

PUD	T_5	T_{50}	T_{max}	wt% Acid	Residual Acid Equivalents
PU-Propanoic	209 ± 6	320 ± 1	313 ± 1	8.2 ± 0.4	1.1
PU-Acrylic	172 ± 1	328 ± 3	323 ± 4	10.0 ± 0.3	1.3
PU-Lactic	151 ± 3	311 ± 1	323 ± 4	15.8 ± 0.3	1.5
PU-Isobutyric	180 ± 3	320 ± 1	313 ± 1	10.8 ± 0.2	1.2

Dynamic Mechanical Analysis. The mechanical properties of all of the PU films have been investigated by dynamic mechanical analysis. For PU films neutralized with different chain length carboxylic acids, the resulting storage modulus (E') and tan delta curves are shown in Figure 5a and 4b, respectively. At low temperatures, the cationic coatings are glassy. The storage modulus decreases rapidly in the temperature range from 20 – 50 °C. The tan delta peaks are recorded as T_g values in Table 3. Generally, the storage modulus at room temperature (Table 3) and T_g decreases as the carboxylic acid chain length increases.

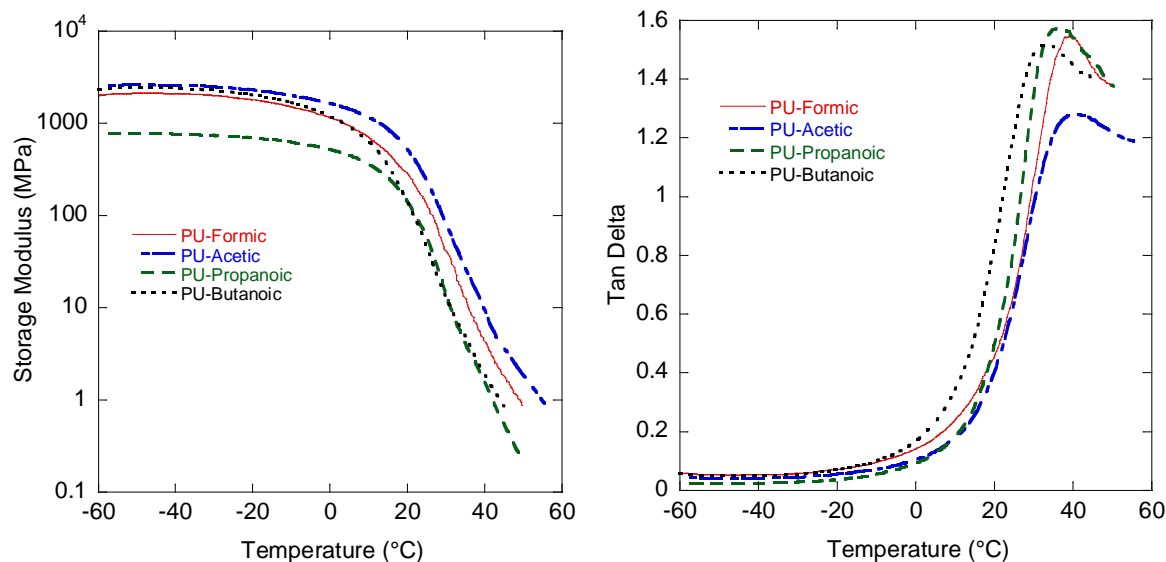


Figure 5. DMA curves for PU films neutralized with different chain length carboxylic acids. a) Storage modulus versus temperature, and b) Tan delta versus temperature.

Table 3: DSC and DMA data for PU films neutralized with different chain length carboxylic acids

PU Film	T_g^a (°C)	T_g^b (°C)	E' at 25 °C (MPa)
PU-Formic	39.7	4.4	132.5
PU-Acetic	40.1	2.4	242.6
PU-Propanoic	36.8	-2.8	57.9
PU-Butanoic	33.7	-2.9	44.6

^a Glass transition temperature obtained from DMA analysis.

^b Glass transition temperature obtained from DSC analysis

Figure 6 shows the storage modulus-temperature curves and the tan delta curves for PU films neutralized with carboxylic acids containing different substituents. The DMA data is summarized in Table 4. The values for the storage modulus at room temperature indicate that the sharp drop in the storage modulus for the PU-Lactic and PU-Acrylic films is shifted to higher temperatures. The PU-Lactic and PU-Acrylic films also exhibit higher T_g values than the PU-Propanoic film. The increased T_g value for the PU-Lactic film is consistent with

the presence of hydrogen bonding by the counterion. The T_g value for the PU-Isobutyric film is slightly lower than the T_g for the PU-Propanoic film, which can be attributed to steric contributions of the counterion.

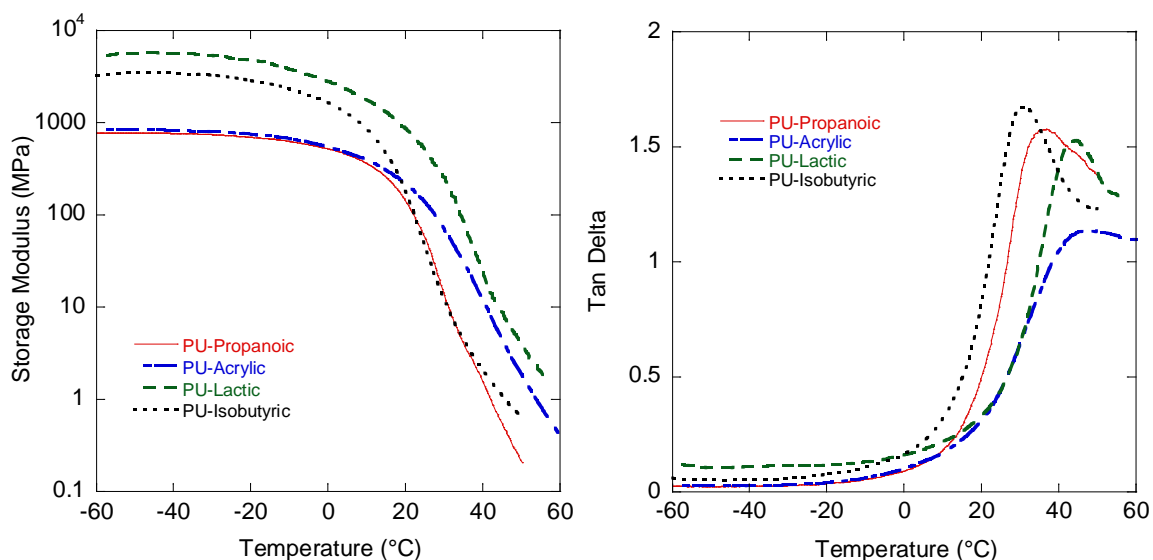


Figure 6. DMA curves for PU films neutralized with carboxylic acids containing different substituents. a) Storage modulus versus temperature and b) Tan delta versus temperature

Table 4. DSC and DMA data for PU films neutralized with carboxylic acids containing different substituents.

PU Film	T_g^a (°C)	T_g^b (°C)	E' at 25 °C (MPa)
PU-Isobutyric	36.32	-3.2	45.9
PU-Propanoic	36.82	-2.8	57.9
PU-Acrylic	48.1	2.0	139.1
PU-Lactic	44.4	10.5	517.8

^a Glass transition temperature obtained from DMA analysis.

^b Glass transition temperature obtained from DSC analysis

Differential Scanning Calorimetry. The T_g values obtained by DSC analyses are lower than those obtained from the DMA tan delta peaks due to inherent differences in the two

techniques.³¹ The T_g values obtained from DSC follow the same general trends as observed by DMA for all of the PU films. The T_g values for PU films neutralized with different chain length carboxylic acids and for PU films neutralized with carboxylic acids containing different substituents are listed in Tables 3 and 4, respectively. The DSC curves for all of the PU films are shown in Figure 7.

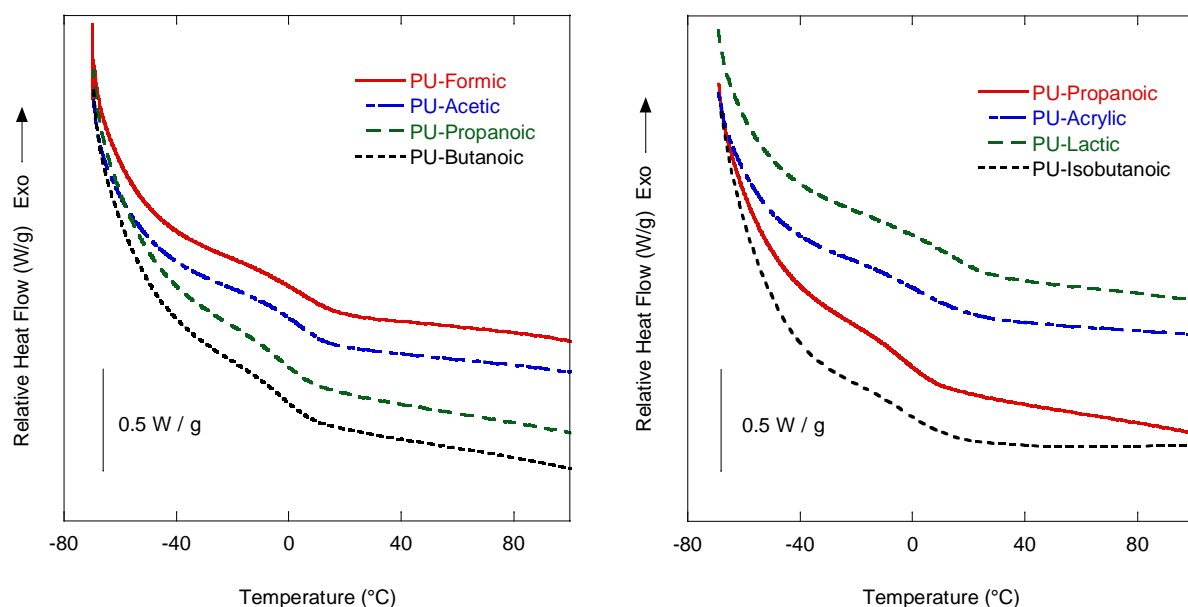


Figure 7. DSC curves for a) PU films neutralized with different chain length carboxylic acids and b) PU films neutralized with carboxylic acids containing different substituents

Conclusions

Castor oil-based cationic polyurethane dispersions (PUDs) have been prepared by neutralizing the intermediate amines with seven different carboxylic acids. Increases in the chain length of the counterions slightly decrease the T_g values of the PU films. Substituents on the counterion appear to have a larger impact than the carbon chain length. In particular, hydrogen bonding increased the T_g value and storage modulus at room temperature of the PU-Lactic films. After initial decomposition, the thermal stabilities of all of the PU films

were very similar. However, the PU-Lactic film exhibited significantly lower initial thermal stability due to excess water and residual acid in the film. Promising results from the preliminary antimicrobial testing conducted (data not shown) indicate that selection of the counterion plays a role in the antimicrobial properties of the cationic PU films. This work will be submitted for publication after the antimicrobial testing is completed.

Acknowledgements

We gratefully acknowledge financial support from the Consortium for Plant Biotechnology Research (CPBR) and the Archer Daniels Midland (ADM) Company. We also thank Dr. Quentin Lineberry of the Institute for Combustion Science & Environmental Technology at Western Kentucky University for his assistance with the TG-MS measurement.

References

1. D.-K. Lee, H.-B. Tsai, H.-H. Wang and R.-S. Tsai, *J. Appl. Polym. Sci.*, 2004, **94**, 1723.
2. B. K. Kim, T. K. Kim and H. M. Jeong, *J. Appl. Polym. Sci.*, 1994, **53**, 371.
3. K.-L. Noble, *Prog. Org. Coat.*, 1997, **32**, 131.
4. A. Overbeek, *J. Coat. Technol. Res.*, 2010, **7**, 1.
5. Y. S. Kwak, S. W. Park and H. D. Kim, *Colloid Polym. Sci.*, 2003, **281**, 957.
6. H. Rajan, P. Rajalingam and G. Radhakrishnan, *Polym. Commun.*, 1991, **32**, 93.
7. B. K. Kim, *Colloid Polym. Sci.*, 1996, **274**, 599.
8. I. W. Cheong, M. Nomura and J. H. Kim, *Macromol. Chem. Phys.*, 2000, **201**, 2221.
9. J.-E. Yang, J.-S. Kong, S.-W. Park, D.-J. Lee and H.-D. Kim, *J. Appl. Polym. Sci.*, 2002, **86**, 2375.
10. J. Bullermann, S. Friebe, T. Salthammer and R. Spohnholz, *Prog. Org. Coat.*, 2013, **76**, 609.
11. B. K. Kim and Y. M. Lee, *Colloid Polym. Sci.*, 1992, **270**, 956.
12. G. N. Mahesh, P. Banu and G. Radhakrishnan, *J. Appl. Polym. Sci.*, 1997, **65**, 2105.
13. G. N. Manvi and R. N. Jagtap, *J. Disper. Sci. Technol.*, 2010, **31**, 1376.
14. O. Jaudouin, J. J. Robin, J. M. Lopez-Cuesta, D. Perrin and C. Imbert, *Polym. Int.*, 2012, **61**, 495.

15. D. J. Hourston, G. D. Williams, R. Satguru, J. C. Padget and D. Pears, *J. Appl. Polym. Sci.*, 1999, **74**, 556.
16. Y. Chen and Y.-L. Chen, *J. Appl. Polym. Sci.*, 1992, **46**, 435.
17. K. Mequanint, R. Sanderson and H. Pasch, *Polym. Degrad. Stabil.*, 2002, **77**, 121.
18. H. A. Al-Salah, K. C. Frisch, H. X. Xiao and J. A. McLean, *J. Polym. Sci. Pol. Chem.*, 1987, **25**, 2127.
19. F. Chen, J. Hehl, Y. Su, C. Mattheis, A. Greiner and S. Agarwal, *Polym. Int.*, 2013.
20. Y. Xia, Z. Zhang, M. R. Kessler, B. Brehm-Stecher and R. C. Larock, *ChemSusChem*, 2012, **5**, 2221.
21. Y. Gao and I. L. Kyratzis, *J. Appl. Polym. Sci.*, 2012, **125**, E71.
22. X. H. Yan, Y. X. Ji and T. He, *Prog. Org. Coat.*, 2013, **76**, 11.
23. A. G. Charnetskaya, G. Polizos, V. I. Shtompel, E. G. Privalko, Y. Y. Kercha and P. Pissis, *Eur. Polym. J.*, 2003, **39**, 2167.
24. P. Krol and B. Krol, *Colloid Polym. Sci.*, 2008, **286**, 1111.
25. B. Krol and P. Krol, *Colloid Polym. Sci.*, 2009, **287**, 189.
26. T. F. Garrison, Z. Zhang, D. Mitra, Y. Xia, D. P. Pfister, B. F. Brehm-Stecher, R. C. Larock and M. R. Kessler, unpublished work.
27. Z. S. Petrović, Z. Zavargo, J. H. Flynn and W. J. Macknight, *J. Appl. Polym. Sci.*, 1994, **51**, 1087.
28. NIST Mass Spec Data Center and S. E. Stein, in *NIST Chemistry WebBook, NIST Standard Reference Database Number 69*, eds. P. J. Linstrom and W. G. Mallard, National Institute of Standards and Technology, Gaithersburg, MD, 2011.
29. P. Crews, J. Rodriguez and M. Jaspars, *Organic Structure Analysis*, Oxford University Press, Oxford, 1998.
30. Y.-W. In, J.-J. Kim, H.-J. Kim and S.-W. Oh, *J. Food Safety*, 2013, **33**, 79.
31. Y. Lu, L. Weng and X. Cao, *Carbohydr. Polym.*, 2006, **63**, 198.

CHAPTER 5. GRAFTED HYBRID LATEXES FROM CASTOR OIL-BASED WATERBORNE POLYURETHANES

A paper to be submitted to *Macromolecular Rapid Communications*

Thomas F. Garrison¹, Daniel P. Pfister¹, Mahendra Thunga², Michael R. Kessler*^{2,3}, and Richard C. Larock*¹

¹ Department of Chemistry, Iowa State University, Ames, Iowa

² Department of Materials Science and Engineering, Iowa State University, Ames, Iowa

³ Ames Laboratory, US Dept. of Energy, Ames, Iowa.

Abstract

In this article, recent developments of grafted hybrid latexes are reviewed. We also report our recent investigation of using 2-hydroxyethyl acrylate (HEA) to introduce graft sites for the synthesis of grafted hybrid latexes from castor oil-based waterborne polyurethane dispersions by emulsion graft copolymerization of vinyl monomers. The thermo-physical properties have been investigated using dynamic mechanical analysis and differential scanning calorimetry. Increased ratios of HEA in the grafted hybrid latexes, increase the elongation at break and glass transition temperature. The morphologies of the grafted hybrid latex particles examined by transmission electron microscopy exhibit a hybrid structure instead of a core-shell structure. The elastic properties of the materials were also modeled with Mooney-Rivlin plots to determine cross-link density.

Introduction

Conventional solvent-borne polyurethanes have been widely adopted commercially because of their appearance and high performance characteristics, such as high tensile strength, abrasion resistance, chemical resistance, and toughness.^{1,2} One drawback of conventional solvent-borne polyurethanes is due to environmental impact from emissions of

volatile organic compounds (VOCs) both during processing and during the application lifetime.¹

Waterborne polyurethane dispersions are widely used polymers with a diverse range of applications, including paints, inks, coatings, adhesives, paper and textiles.^{3,4} Polyurethane dispersions are an effective method of reducing the emission of volatile organic compounds generated by organic solvents.^{1,3,4} Although this approach has been used commercially since the late 1960s, waterborne polyurethane dispersions is still a very active area of research.⁵⁻¹⁰ In comparison with other waterborne coatings, polyurethane dispersions have the lowest amounts of organic solvent emissions with amounts as low as 3 wt %. In fact, the low organic solvent emissions of polyurethane dispersions are comparable to the low emission levels typical of powder coatings, which typically range from 0.1 to 4 wt%.¹¹ Polyurethane dispersions offer other advantages, including excellent processability and good film forming properties. One particularly important property for processing is the fact that the viscosity of polyurethane dispersions is almost independent of the molecular weight of the polymer.^{3,12} This allows for the preparation of dispersions with high solid content loadings of high molecular weight polymers, yielding good coatings by physical drying processes.¹³ However, polyurethane dispersions are not without disadvantages, which include high cost, slow drying rates, and poor water and alkali resistance.^{12,14}

Another drawback of conventional solvent-borne polyurethanes is their dependence on a petroleum-based polymers and solvents. In response to the dual concerns about dwindling petroleum reserves and VOC emissions, waterborne polyurethane dispersions have been prepared using biorenewable-based polyols, such as vegetable oils or fatty acids.^[6,15-18]

Hybrid polymeric materials have been synthesized as strategy of overcoming the aforementioned deficiencies of polyurethane dispersions and other polymers. Often, hybrid polymers refer to polymers covalently bonded to inorganic materials or polymers with encapsulated nanoparticles.¹⁹⁻²¹ However, hybrid polymer systems can also include two or more different types of polymers that are normally incompatible, such as thermosets and thermoplastics.¹⁹ Of particular interest, are hybrid latexes made from polyurethanes and acrylics.²² The combination of polyurethane dispersions and acrylic latexes results in significant improvements compared to either individual type of polymer.¹³ Acrylic resins have a number of advantages, including good weatherability, chemical resistance, gloss, and affinity to pigments.²³ However, acrylic resins often exhibit poor toughness, elongation, mar-resistance, and adhesion.²³ Hybrid polyurethane latexes offer the potential of combining the advantages of both acrylic latexes and waterborne polyurethane dispersion systems, while offering lower cost and good affinity to pigments.^{23,24}

A number of different approaches exist for making hybrid materials. Blending is the simplest route and most common method used industrially, where mixtures of polyurethanes and acrylic polymers are not covalently bonded to each other.^{13,22,25} However, the improved performance is obtained when the different polymers are covalently attached together. This has been achieved by cross-linking, mini-emulsion, and seeded emulsion.^{22,25,26} Hybrid latexes prepared from mini-emulsion and seeded emulsion polymerization have been reviewed extensively.^{19,27} In mini-emulsion, polycondensate or polyaddition polymers, such as polyesters, alkyd resins, or polyurethanes, are dissolved in radically polymerizable monomer(s).¹⁹ In seeded emulsion polymerization, a modified polycondensate polymer first

forms a latex in the presence of water, and this latex is used as a seed in an emulsion polymerization of suitable monomers.^{19,23,24,28}

Waterborne polyurethane hybrid latexes is an area of particular interest in waterborne coatings research.^{14,16-18,29-31} These materials are formed by seeded emulsion, by first preparing polyurethane dispersions (step-growth thermosets), followed by polymerization of vinyl monomers (chain growth thermoplastics). Previously, our group has reported the synthesis of vegetable oil-based urethane-acrylic latexes.^{9,16,32} In one study, acrylic polymer chains were grafted onto the polyurethane chains by reacting them with the carbon-carbon double bonds in the fatty acids.¹⁶ In another study, grafted latexes were prepared using acrylated epoxidized soybean oil to introduce vinyl groups into the polyurethane chains for subsequent emulsion graft copolymerization with mixtures of butyl acrylate and methyl methacrylate.³² More recently, our group reported curing castor oil-based waterborne polyurethane dispersions with an aziridine-based crosslinker.³³

In the present work, 2-hydroxyethyl acrylate (HEA) has been incorporated into castor oil-based polyurethane dispersions as a precursor to making grafted hybrid latex dispersions from waterborne castor oil-based polyurethane dispersions.³⁴ It is well known that HEA can be used used to introduce hydroxyl groups for cross linking sites in acrylic latexes.¹³ However, the objective of this work is to investigate the use of HEA as a means of introducing vinyl groups for grafting in the preparation of castor oil-based grafted hybrid latexes (GHL). The advantage of using castor oil and HEA over acrylated soybean oil is that it eliminates the need for additional processing of soybean oil oil by epoxidation and ring opening with acylated groups. The effect of different molar ratios of vinyl monomers (styrene and butyl acrylate) on the resulting GHL was also examined. Recently, styrene and

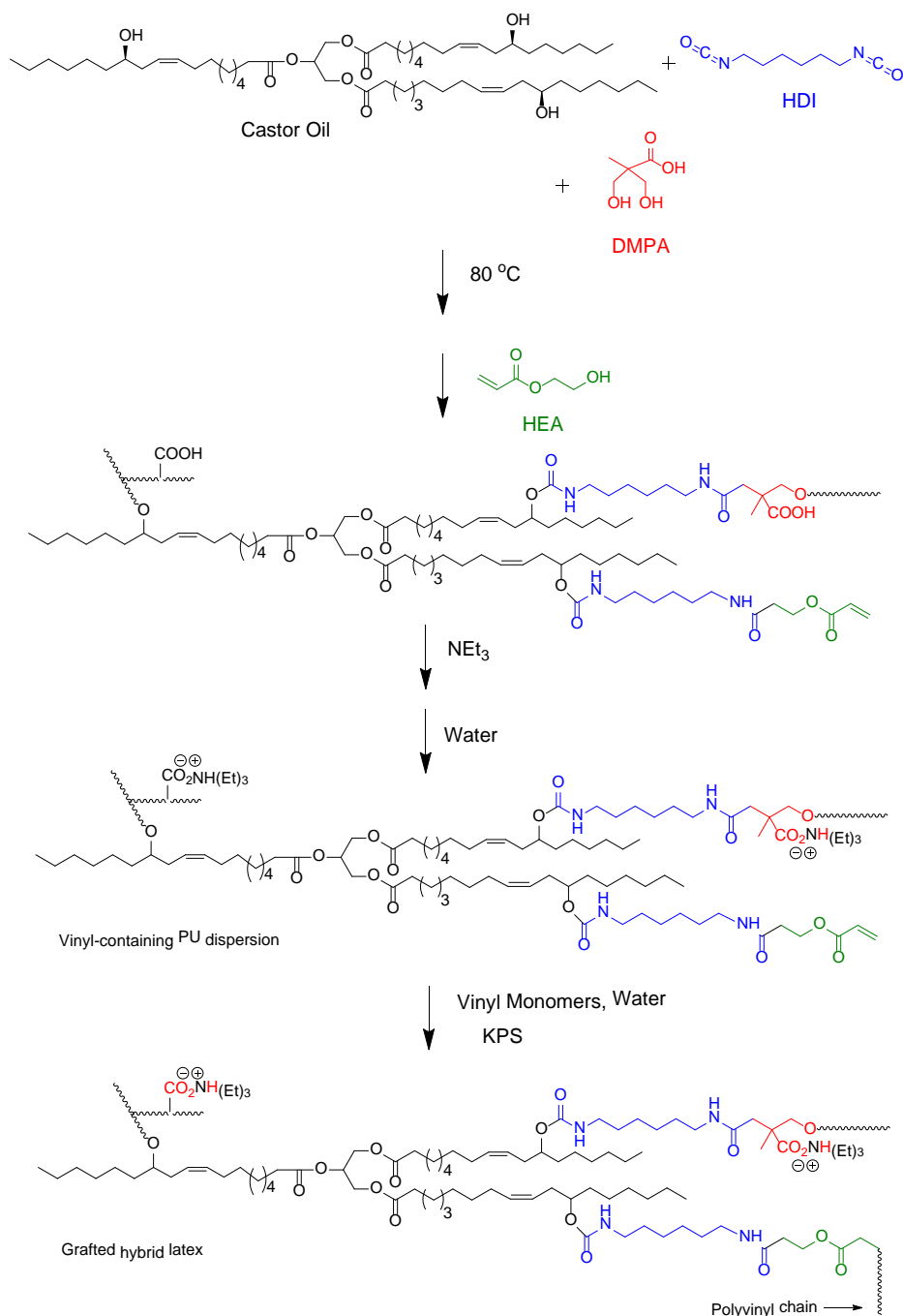
butyl acrylate were used to prepare hybrid polyurethane latexes from polyester-based polyurethanes, which showed excellent properties as a paper surface sizing agent in papermaking.³⁵ The morphology and properties of these GHs have subsequently been investigated using transmission electron microscopy, mechanical testing, dynamic mechanical analysis, differential scanning calorimetry, and thermogravimetry. Mooney Rivlin plots were used to determine molecular weight between cross-links.

Experimental

Materials. Castor oil, dimethylolpropionic acid (DMPA), hexamethylene diisocyanate (HDI), dibutyltin dilaurate (DBTDL), 2-hydroxyethyl acrylate (HEA), butyl acrylate, and styrene were purchased from Aldrich Chemical Company (Milwaukee, WI, USA). Glacial acetic acid, methyl ethyl ketone, triethylamine, and potassium persulfate (KPS) were purchased from Fisher Scientific Company (Fair Lawn, NJ, USA). All materials were used as received.

Synthesis of the castor oil-based grafted hybrid latexes. Scheme 1 illustrates the synthesis of our castor oil-based grafted hybrid latexes. HDI, dimethylolpropionic acid, castor oil, and one drop of DBTDL were added to a three-necked flask equipped with a mechanical stirrer, condenser, and a thermometer. The molar ratio between the NCO groups of IPDI, the OH groups of castor oil, the OH groups of DMPA, and the OH groups of HEA is listed in Table 1. The reaction was heated at 80 °C for 1 h. HEA was added to end-cap the polyurethane chains with vinyl groups and methyl ethyl ketone (50 wt % based on the total reactants) was added to reduce the viscosity. After 3 h of additional reaction, the reactants were cooled to room temperature and triethylamine (1.5 equivalents) was added, followed by dispersion at high speed with distilled water to produce anionic, vinyl-containing PUDs with a solid

content of ca. 10 wt % after removal of the methyl ethyl ketone under vacuum. The molar ratio of NCO groups from HDI and the molar ratio of OH groups from DMPA were held constant. As the molar ratio of OH groups from castor oil was decreased, the molar ratio of OH groups from HEA was correspondingly increased.



Scheme 1. Synthesis of castor oil-based grafted hybrid latexes

Table 1. Chemical composition of PU and GHL films

Sample	Molar Ratio				Vinyl Monomers (wt %)
	NCO (IPDI)	OH ^a	OH ^b	OH ^c	
PU-0.0	2.0	1.0	0.99	0.0	0
PU-0.1	2.0	0.9	0.99	0.1	0
PU-0.2	2.0	0.8	0.99	0.2	0
PU-0.3	2.0	0.7	0.99	0.3	0
GHL-0.0	2.0	1.0	0.99	0.0	30
GHL-0.1	2.0	0.9	0.99	0.1	30
GHL-0.2	2.0	0.8	0.99	0.2	30
GHL-0.3	2.0	0.7	0.99	0.3	30

^a Hydroxyl molar ratio of the castor oil, ^b Hydroxyl molar ratio of the DMPA, ^c Hydroxyl molar ratio of the HEA

To prepare the grafted hybrid latexes, the vinyl monomers and distilled water were added to the vinyl-containing polyurethanes and stirred under argon gas for 2 h. After flushing with argon, potassium persulfate was added and the reaction mixture was heated to 80 °C. The reaction was allowed to proceed for 4 h before cooling to room temperature. The composition of the grafted hybrid latex was 70 wt % polyurethane and 30 wt % vinyl monomers (butyl acrylate and styrene). Unless otherwise mentioned, the ratio of butyl acrylate : styrene was held at 1 : 1. In order to determine the effect of varying the vinyl monomer ratio on the thermal properties of the resulting GHLs, butyl acrylate : styrene ratios of 3 : 1 and 1 : 3 were also investigated.

The PU films are identified as PU-0.0, PU-0.1, PU-0.2, and PU-0.3, where the number represents the molar ratio of HEA. The grafted hybrid latex films are identified as GHL-0.0, GHL-0.1, GHL 0.2, and GHL-0.3, where the number corresponds to the molar ratio of HEA. The corresponding vinyl-containing polyurethane films and GHL films have been obtained by drying the resulting dispersions at room temperature in polystyrene petri dishes.

Characterization. The grafted hybrid latex particle morphology has been studied under a transmission electron microscope (JEOL-2100). The latexes were diluted with deionized water, and one drop of the diluted emulsion was placed on the coated side of a 200-mesh nickel grid in a petri dish. After drying, the samples were stained with osmium tetroxide and characterized. The mechanical properties of the vinyl-containing polyurethanes and grafted hybrid latex films were determined using an Instron universal testing machine (Model-4502). The crosshead speed was set at 100 mm/min. Average stress-strain data gained from five rectangular specimens (70 mm × 10 mm) were used. The dynamic mechanical behavior of the vinyl-containing polyurethanes and grafted hybrid latex films was determined using a dynamic mechanical analyzer (TA Instruments DMA Q800, New Castle, DE) in tensile mode at 1 Hz. The samples were heated from -80 to 100 °C at a rate of 5 °C/min. The glass transition temperatures (T_g) were obtained from the $\tan \delta$ peaks. Differential scanning calorimetry (DSC) was performed using a differential scanning calorimeter (TA Instruments DSC Q20, USA). The samples were heated from 25 to 100 °C at a rate of 20 °C/min to erase their thermal history, cooled to -70 °C, and heated again to 150 °C at a heating rate of 20 °C/min. The sample mass was approximately 5 mg. A thermogravimetric analyzer (TA Instruments TGA Q50, USA) was used to measure the weight loss of the vinyl-containing polyurethanes and grafted hybrid latex films in an air atmosphere. The samples were heated from 30 to 650 °C at a heating rate of 20 °C/min. The mass of the samples used for TGA analysis was approximately 8 mg.

Results and Discussion

TEM Microscopy. The transmission electron microscopy images of the polyurethane particles and grafted hybrid latex particles, shown in Figure 1, illustrate the change in particle morphology based on HEA ratio. For the PUDs, the particles were spherical or oblong and relatively hard to observe in comparison to the grafted hybrid latex particles (Figure 1a). In contrast, the grafted hybrid latexes with HEA molar ratios 0.2 or less (Figure 1b), showed clearly defined spherical particles typically larger than 200 nm in size. However, the GHL-0.3 particles (Figure 1c) were much smaller (less than 100 nm), exhibited more irregular shapes, and were more disperse than those observed for GHL-0.2. The transition in observed morphology from GHL-0.2 to GHL-0.3 indicates a change in polymer structure, which can possibly be attributed to a decreased molecular weight of the polyurethane backbone due to an excess of HEA. When HEA is incorporated into a step growth polymer, it also acts as a chain terminator, in addition to being a graft site for the subsequent grafting of acrylic polymer chains. The observed morphology changes are consistent with the results of the thermomechanical testing.

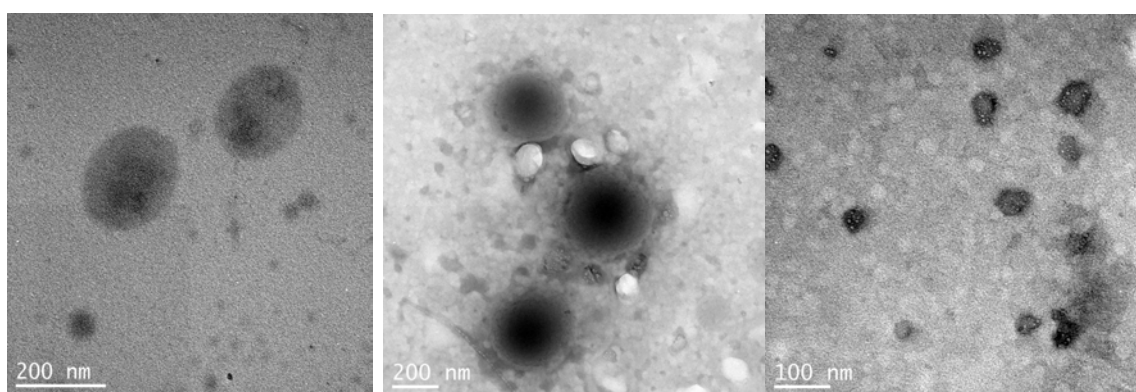


Figure 1. TEM microphotographs of particles from the PU-0.0 dispersion (a) and grafted latexes of GHL-0.2 (b) and GHL-0.3 (c).

The morphology of the GHL-0.2 particles also exhibits a hybrid structure, instead of a core-shell structure. In a core-shell structure, there are clearly defined layers with a hydrophobic core and a hydrophilic shell.^[9] However, in the GHL-0.2 particles, the broad distribution of osmium tetroxide stain indicates that the grafted latex particles have a hybrid structure, instead of a core-shell structure. The osmium tetroxide preferentially reacts with the carbon-carbon double bonds that are only found in the castor oil-based polyurethane chains. This indicates that the particle interior is a hybrid mixture of grafted polyvinyl chains and polyurethane chains, whereas the particle surface is covered with the hydrophilic anionomer groups incorporated into the polyurethane chains.

Mechanical Properties. The tensile test results for the vinyl-containing polyurethanes and the grafted hybrid latex films are summarized in Table 2. For the vinyl-containing polyurethane films, the tensile strength decreased, while the elongation at break increased as the molar ratio of HEA increased from 0.0 to 0.2. PU-0.3 had a higher Young's modulus and toughness compared to the other vinyl-containing polyurethane films, as well as greater variability in the toughness and elongation at break. For the grafted hybrid latex films, the tensile strength decreased from 2.56 MPa to 1.21 MPa as the HEA increased from 0.0 to 0.3, but it improved relative to the corresponding vinyl-containing polyurethane. The Young's modulus of the grafted latexes increased from 1.79 to 4.39 MPa as the HEA molar ratio increased from 0.0 to 0.3. The elongation at break remained relatively constant as the HEA increased, but decreased slightly as the HEA molar ratio increased from 0.2 to 0.3. It should be noted that for both the vinyl-containing polyurethanes and the grafted hybrid latexes, the decrease in break strength and elongation at break observed as the HEA molar ratio increased from 0.2 to 0.3 is consistent with the changes in particle morphology.

Table 2. Summary of engineering stress data

Film	HEA Molar Ratio	σ_b (MPa) ^{a)}	E (MPa) ^{b)}	Toughness (MPa)	ϵ_b (%) ^{c)}
PU	0.0	1.57 ± 0.10	1.01 ± 0.19	2.31 ± 0.17	319 ± 12
	0.1	1.49 ± 0.21	0.97 ± 0.11	2.97 ± 0.47	435 ± 34
	0.2	0.88 ± 0.06	1.01 ± 0.13	2.16 ± 0.10	560 ± 19
	0.3	1.16 ± 0.11	1.75 ± 0.11	3.85 ± 0.68	539 ± 69
GHL	0.0	2.56 ± 0.17	1.79 ± 0.10	4.61 ± 0.39	396 ± 18
	0.1	2.10 ± 0.17	2.50 ± 0.20	3.98 ± 0.34	396 ± 14
	0.2	1.61 ± 0.06	2.50 ± 0.32	3.08 ± 0.13	401 ± 10
	0.3	1.21 ± 0.10	4.39 ± 0.27	3.08 ± 0.24	364 ± 13

^{a)} σ_b is break strength, ^{b)} E is Young's modulus, ^{c)} ϵ_b is the strain at break

The Mooney-Rivlin equation, as shown in Equation 1, can be used to estimate the molecular weight between crosslinks (M_c) from the stress-strain behavior as shown in Equation 2, where σ is the tensile stress, λ is the stretch ratio, C1 and C2 are experimentally determined parameters, ρ is the density of the polymer, R is the gas constant, and T is the absolute temperature.^[36, 37]

$$\text{Equation 1.} \quad \sigma = \left(2C_1 + \frac{2C_2}{\lambda} \right) \left(\lambda - \frac{1}{\lambda^2} \right)$$

$$\text{Equation 2:} \quad 2C_1 = \frac{\rho RT}{M_c}$$

The tensile data conforms to Equation 1, as shown in Figure 2. The values for M_c are listed in Table 3. The crosslink density is inversely proportional to M_c . For the vinyl-containing polyurethane films, M_c increased with increasing amounts of HEA, whereas for the grafted hybrid latex films, M_c did not change as the HEA molar ratio increased from 0.2 to 0.3. The model was not applied to the samples PU-0.3 and GHL-0.3 with the highest

amounts of HEA, because of changes in the morphology and behavior. Figure 2 illustrates that there was an absence of a rubbery plateau for PU-0.3.

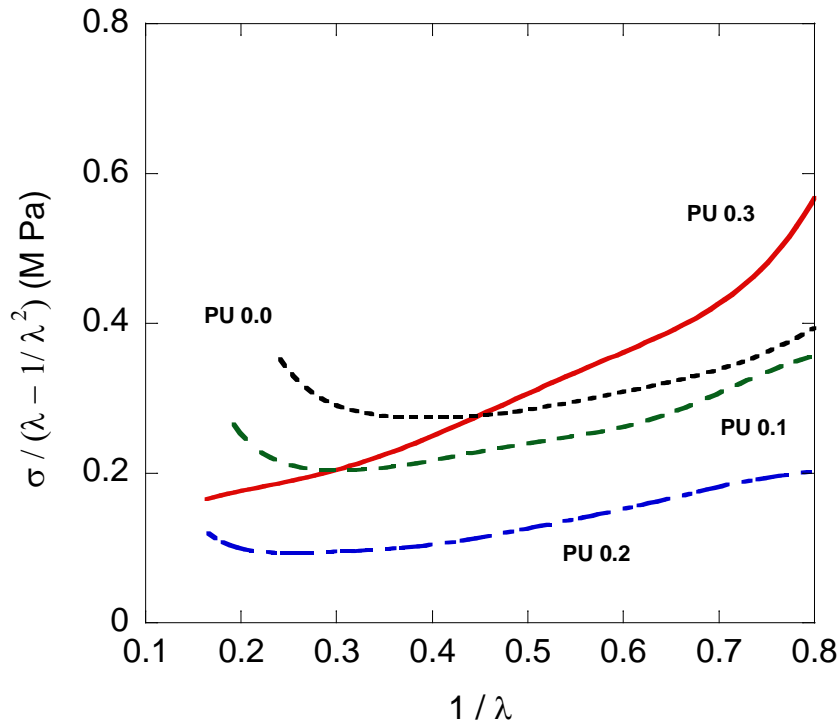


Figure 2. Mooney-Rivlin plot for PU films with different molar ratios of HEA.

Table 3. Molecular weight between crosslinks (M_c) estimated from Mooney-Rivlin plots

PU Film	M_c (kg / mol)	GHL Film	M_c (kg / mol)
PU 0.0	5.9	GHL 0.0	4.8
PU 0.1	9.3	GHL 0.1	8.2
PU 0.2	16.1	GHL 0.2	8.1
PU 0.3	n/a	GHL 0.3	n/a

Thermal Properties. The storage modulus (E') of both the vinyl-containing polyurethanes and the grafted hybrid latex films are shown in Figure 3 and 4, respectively. The storage

modulus of the vinyl-containing polyurethanes decreased as the ratio of HEA increased. This can be attributed to HEA causing more chain termination, leading to more dangling chains. The decrease in storage modulus also results from the decreased cross-link density. In contrast, the storage modulus increased for the grafted latexes as the ratio of HEA increased, which can be explained by the relative decrease in castor oil, which makes the polymer chains less flexible.

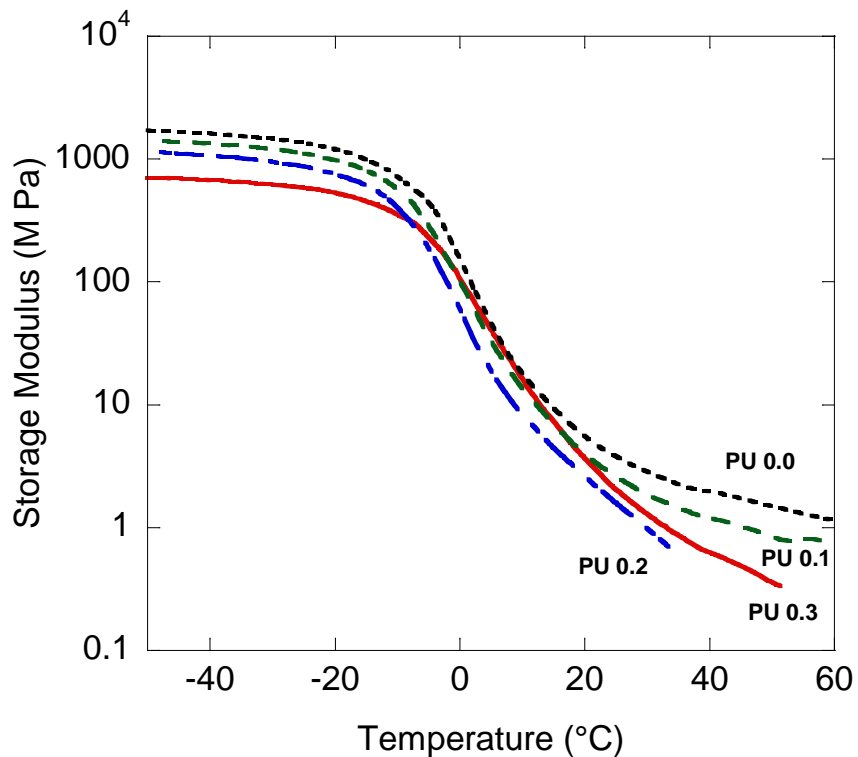


Figure 3. Storage modulus as a function of temperature for polyurethane films with different amounts of HEA

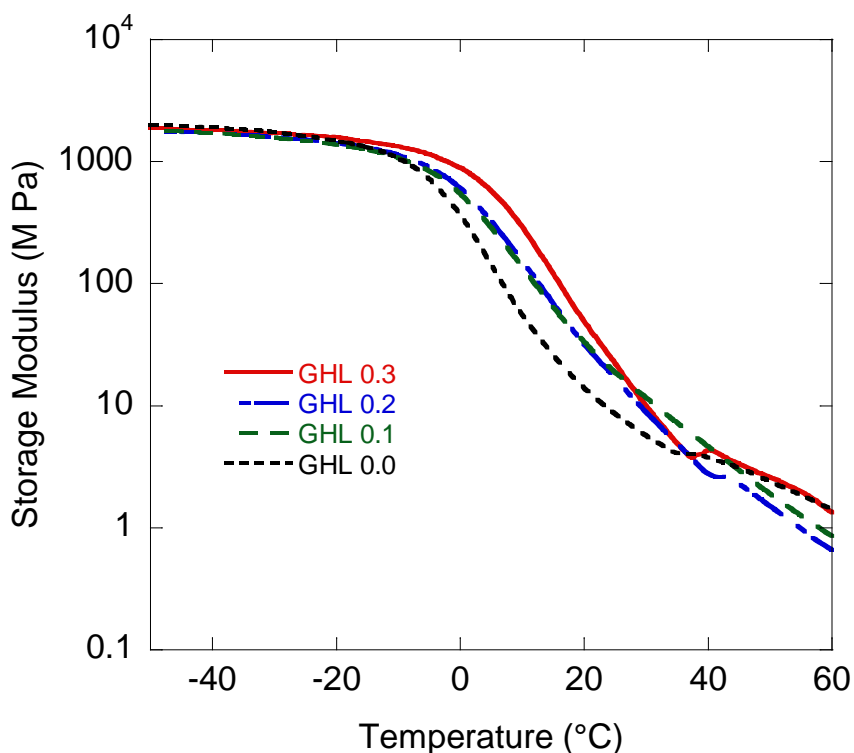


Figure 4. Storage modulus as a function of temperature for grafted hybrid latex films with different amounts of HEA

The glass transition temperatures, T_g 's, of both the vinyl-containing polyurethanes and the grafted hybrid latexes have been determined using DMA and DSC, as summarized in Table 4. With DMA, the $\tan \delta$ peak corresponds to the relaxation processes of the polymers and is a measure of T_g . DSC determines the T_g by measuring changes in the heat capacity between the glassy and rubbery states. Both methods exhibit similar trends. However, the T_g determined by DSC is lower than the T_g determined by the $\tan \delta$ peak in the DMA. The T_g of the vinyl-containing polyurethanes decreased as the ratio of the HEA increased from 0.0 to 0.2 and then increased only slightly as the ratio of the HEA increased from 0.2 to 0.3. In contrast, the T_g of the grafted hybrid latexes increased as the ratio of the HEA increased,

which indicates improved grafting of the vinyl monomers. In addition, the presence of single glass transitions is an indication of a grafted latex as opposed to a physical polymer blend.³²

Table 4. Summary of thermal properties

Film	HEA Molar Ratio	T_g (DMA) (°C)	T_g (DSC) (°C)	TGA	
				T_5 (°C)	T_{50} (°C)
PU	0.00	6.28	-18.60	232	373
	0.10	4.88	-20.80	218	361
	0.20	3.80	-21.70	220	359
	0.30	11.46	-19.60	219	357
GHL	0.00	9.36	-19.80	231	391
	0.10	14.92	-16.10	228	392
	0.20	15.98	-9.30	228	403
	0.30	20.31	-4.80	224	413

The thermal stability of the films has been investigated using thermogravimetric analysis (TGA). The two TGA parameters reported in Table 4 are the temperatures of 5% and 50% degradation (T_5 and T_{50} , respectively). The parameter T_5 corresponds to the onset degradation temperature, while the parameter T_{50} corresponds to the mid-point temperature of degradation. Both the vinyl-containing polyurethanes and the grafted hybrid latexes exhibit a similar trend with T_5 degradation temperatures that slightly decrease as the ratio of the HEA increases. However, T_{50} decreased as the ratio of the HEA increased for the vinyl-containing polyurethanes, while for the grafted hybrid latexes, T_{50} increased with the HEA ratio. The increase in T_{50} for the grafted hybrid latexes indicates that grafting improves the thermal stability.

Vinyl monomer composition. Styrene and butyl acrylate are two common monomers used in the synthesis of commercial latex emulsions. Styrene is typically used to reduce cost and impart hardness to the dried film, whereas butyl acrylate is used to add flexibility. For the grafted hybrid latexes, the thermal properties of two additional monomer compositions have been examined, namely butyl acrylate : styrene ratios of 3 : 1 and 1 : 3, in addition to the 1 : 1 data presented above. As expected, the butyl acrylate-rich grafted hybrid latex exhibits a lower storage modulus owing to more flexible segments, while the styrene-rich grafted hybrid latex is more rigid, as shown in Figure 5. The vinyl monomer composition did not significantly influence the T_g (data not shown).

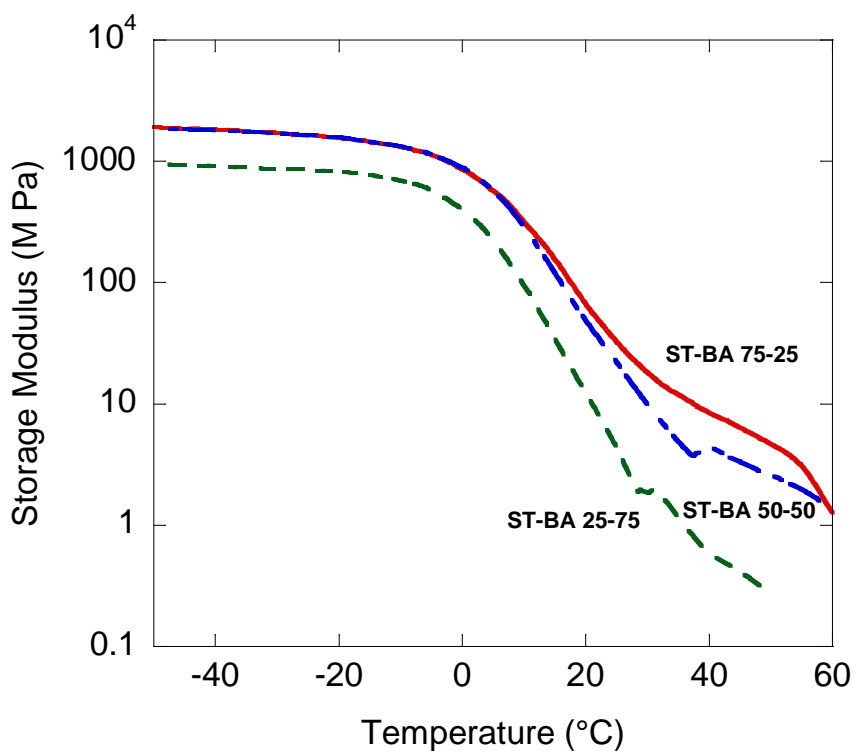


Figure 5. Storage modulus as a function of temperature for GHF-0.3 films with different vinyl monomer compositions

Conclusions

Vinyl-containing waterborne PUDs have been successfully synthesized from castor oil, where HEA has been used to introduce vinyl groups for subsequent grafting. The grafted hybrid latexes prepared exhibit improved thermal and mechanical properties over the vinyl-containing polyurethanes. However, excessive amounts of HEA relative to castor oil significantly change both the morphology and the properties of the grafted hybrid latexes. Generally, it was observed that as the molar ratio of HEA increases from 0.2 to 0.3 and as the molar ratio of castor oil simultaneously decreases, there is a significant change in the particle size, morphology, thermal properties, and mechanical properties. Two competing phenomena likely contribute to the results. Castor oil acts as both a cross-linker and a soft chain supplier, whereas HEA acts as both a chain terminator and as a graft site for polyvinyl chains. Consequently, changes in the relative composition of HEA and castor oil significantly impact the properties of the films.

For the grafted hybrid latexes, increases in the ratio of the HEA improve the properties of the materials. It is also observed that changing the vinyl monomer composition changes the properties of the materials. From these observations, we conclude that both the HEA and vinyl monomer ratios can be tuned to improve the properties of grafted hybrid latexes.

Acknowledgements

We gratefully acknowledge financial support from the Consortium for Plant Biotechnology Research (CPBR) and the Archer Daniels Midland (ADM) Company. We also thank Ms. Tracey M. Pepper of the Microscopy and NanoImaging Facility (MNIF) at Iowa State University for her assistance with the TEM analysis.

References

1. K.-L. Noble, *Prog. Org. Coat.*, 1997, **32**, 131.
2. A. Overbeek, *J. Coat. Technol. Res.*, 2010, **7**, 1.
3. B. K. Kim, *Colloid Polym. Sci.*, 1996, **274**, 599.
4. S. Y. Lee, J. S. Lee and B. K. Kim, *Polym. Int.*, 1997, **42**, 67.
5. S. K. Lee and B. K. Kim, *J. Colloid Interf. Sci.*, 2009, **336**, 208.
6. A. Patel, C. Patel, M. G. Patel, M. Patel and A. Dighe, *Prog. Org. Coat.*, 2010, **67**, 255.
7. Y. Lu and R. C. Larock, *ChemSusChem*, 2010, **3**, 329.
8. Y. Lu and R. C. Larock, *Prog. Org. Coat.*, 2010, **69**, 31.
9. Y. Lu, Y. Xia and R. C. Larock, *Prog. Org. Coat.*, 2011, **71**, 336.
10. V. D. Athawale and R. V. Nimbalkar, *J. Disper. Sci. Technol.*, 2011, **32**, 1014.
11. K. Dören, W. Freitag and D. Stoye, *Water-Borne Coatings: The Environmentally-friendly Alternative*, Hanser Publishers, Munich, 1994.
12. Y. Lu and R. C. Larock, in *Green Polymer Chemistry: Biocatalysis and Biomaterials*, American Chemical Society, 2010, vol. 1043, pp. 87-102.
13. Z. W. Wicks, Jr., F. N. Jones, S. P. Pappas and D. A. Wicks, *Organic Coatings: Science and Technology*, John Wiley & Sons, Inc., Hoboken, NJ, 2007.
14. H. Fu, H. Huang, Q. Wang, H. Zhang and H. C. HQ, *J. Disper. Sci. Technol.*, 2009, **30**, 634.
15. Y. Lu and R. C. Larock, *Biomacromolecules*, 2008, **9**, 3332.
16. Y. Lu and R. C. Larock, *Biomacromolecules*, 2007, **8**, 3108.
17. Y. Xia and R. C. Larock, *Green Chem.*, 2010, **12**, 1893.
18. *United States Pat.*, US 6,166,150, 2000.
19. A. Guyut, K. Landfester, F. J. Schork and C. Wangd, *Prog. Polym. Sci.*, 2007, **32**, 1439.
20. C. K. Weiss and K. Landfester, in *Hybrid Latex Particles*, eds. A. M. VanHerk and K. Landfester, 2010, vol. 233, pp. 185-236.
21. A. P. Zhu, Q. P. Rong and R. Chen, *J. Adhes. Sci. Technol.*, 2010, **24**, 267.
22. A. Lopez, E. Degrandi-Contraires, E. Canetta, C. Creton, J. L. Keddie and J. M. Asua, *Langmuir*, 2011, **27**, 3878.
23. M. Hirose, F. Kadowaki and J. Zhou, *Prog. Org. Coat.*, 1997, **31**, 157.
24. M. Hirose, J. Zhou and K. Nagai, *Prog. Org. Coat.*, 2000, **38**, 27.
25. M. Li, E. S. Daniels, V. Dimonie, E. D. Sudol and M. S. El-Aasser, *Macromolecules*, 2005, **38**, 4183.
26. L. Ragupathy, U. Ziener, G. Robert and K. Landfester, *Colloid Polym. Sci.*, 2011, **289**, 229.
27. A. M. VanHerk and K. Landfester, eds., *Hybrid Latex Particles*, Springer-Verlag Berlin, Berlin, 2010.
28. J. Nicolas, B. Charleux, O. Guerret and S. Magnet, *Angewandte Chemie*, 2004, **116**, 6312.
29. C. Zhang, X. Zhang, J. Dai and C. Bai, *Prog. Org. Coat.*, 2008, **63**, 238.
30. M. Goikoetxea, Y. Reyes, C. M. de las Heras Alarcón, R. J. Minari, I. Beristain, M. Paulis, M. J. Barandiaran, J. L. Keddie and J. M. Asua, *Polymer*, 2012, **53**, 1098.
31. V. D. Athawale and R. V. Nimbalkar, *Pigm. Resin. Technol.*, 2011, **40**, 181.

32. Y. Lu and R. C. Larock, *J. Appl. Polym. Sci.*, 2011, **119**, 3305.
33. Y. Xia and R. C. Larock, *Macromol. Mater. Eng.*, 2011, **296**, 703.
34. X. B. Jiang, X. L. Zhu, Z. G. Zhang, X. Z. Kong and Y. B. Tan, *Chem. Res. Chin. Univ.*, 2011, **27**, 154.
35. Y. H. Guo, S. C. Li, G. S. Wang, W. Ma and Z. Huang, *Prog. Org. Coat.*, 2012, **74**, 248.
36. M. Mooney, *J. Appl. Phys.*, 1940, **11**, 582.
37. M. Thunga, A. Das, L. Häußler, R. Weidisch and G. Heinrich, *Compos. Sci. Technol.*, 2010, **70**, 215.

CHAPTER 6. GENERAL CONCLUSIONS

This dissertation discusses the synthesis and characterization of polyurethane dispersions and films produced from vegetable oil-based polyols. A variety of vegetable oils have been used to prepare bio-based polyols for the preparation of polyurethanes. Applications of the environmentally-friendly coatings include paint binders, adhesives, paper coatings, and textile sizings. Polyurethane dispersions, like other waterborne coatings, are environmentally-friendly due to the reduction of hazardous volatile organic compounds emissions compared to conventional solvent-borne coatings.

In Chapter 2, the effects of residual unsaturation and different ring opening methods on vegetable oil-based anionic polyurethane dispersions have been investigated. Different vegetable oils (peanut, soy, corn, and linseed oil) were partially epoxidized and then completely ring-opened to produce vegetable oil-polyols with approximately 2.7 hydroxyl groups per molecule. The residual unsaturation of the resulting polyols ranged from 0.4 to 3.5 carbon-carbon double bonds per triglyceride molecule. Increasing the residual unsaturation improves the break strength, Young's modulus, and toughness of the polyurethane films. The fatty acid composition of the vegetable oils also impacts the properties of the polyurethanes by changing the distribution of the hydroxyl groups.

The focus of Chapter 3 is on the thermal, mechanical and antimicrobial properties of soybean oil-based cationic polyurethane dispersions. The molar ratio of hydroxyl groups contributed by N-methyl diethanolamine was varied relative to the molar ratio of hydroxyl groups from the soybean polyols. Higher ratios of ammonium cations, which were synthesized by neutralization of the N-methyl diethanolamine, showed increased

antimicrobial activity of the polyurethane films against three food-borne pathogens: *Salmonella typhimurium*, *Listeria monocytogenes*, and *Staphylococcus aureus*.

Chapter 4 continues our investigation into cationic polyurethane dispersions by examining the effects of counterions on the thermal and mechanical properties of the resulting PU films. Previous research into the effect of counterions on cationic polyurethane dispersions has been limited to anionic polyurethane dispersions. Both chain length and chain substituents impact the initial thermal stability, glass transition temperature, and storage modulus of the polyurethane films. After decomposition of the ammonium group, the thermal profiles of all of the polyurethane films were very similar.

Chapter 5 explores the use of 2-hydroxyethyl acrylate as means of introducing graft sites for the synthesis of grafted hybrid latexes from polyurethane dispersions. The elastic properties of the materials have been characterized by tensile testing and the tensile stress/strain curves modeled by the Mooney-Rivlin equation for rubber elasticity revealed the influence of the 2-hydroxyethyl acrylate on the crosslink density. Increased ratios of 2-hydroxyethyl acrylate in the grafted hybrid latexes improved the grafting of the vinyl monomers. Higher ratios of 2-hydroxyethyl acrylate produced films with increased elongation at break and higher glass transition temperatures.

While the vegetable oil-based polyurethane dispersions described in this dissertation show promise for future applications, some challenges remain. Specifically, the percent solids content of these dispersions needs to be higher for a number of applications. Compatibility testing with pigments and additives, as well as adhesion testing to specific substrates, will likely reveal additional hurdles and limitations for these materials. Economic

competitiveness with existing petroleum-based coatings is likely the most significant challenge to the use of bio-based polyurethane coatings.

Long term, the future remains bright for bio-based polyurethanes. These materials can be adapted for uses in higher value products like pressure sensitive adhesives. New approaches to increase the bio-content in polyurethanes are being pursued by the development of bio-based isocyanates. The residual unsaturation of vegetable oil-based polyols can be used either for additional functionalization or UV curing. Demand for inexpensive antimicrobial coatings for food packaging applications will continue to grow. While bio-based polyurethanes will not completely replace petroleum-based coatings, these materials will continue to find uses in a wide range of applications.

ACKNOWLEDGEMENTS

I would like to express my deepest appreciation to my co-major advisors, Distinguished Professor Emeritus Richard C. Larock and Professor Michael R. Kessler, who have guided me through my Ph.D. studies. I am very grateful for their guidance, support, and encouragement.

I sincerely appreciate my Program of Study committee members; Dr. Malika Jeffries-El, Dr. Arthur Winter, and Dr. Keith Woo for their valuable time and support during my studies at Iowa State University.

I want to thank my many colleagues in Dr. Larock's group and in Dr. Kessler's group, past and present, for their friendship. In particular, I thank Dr. Yongshang Lu, Dr. Ying Xia, Dr. Dan Pfister, Dr. Rafael Quirino, Dr. Anton Dubrovsky, Dr. Peter Hondred, and Daniel Vennerberg for their assistance and insightful discussions. I have enjoyed working with all of you.

I would like to thank my friends and family. I have been blessed with wonderful friends and relatives who have aided me through the years with kind words of encouragement. Finally, I thank my wife Andrea, because I could not have done this without her steadfast love and support.

This research was funded in part by the CPBR and Archer Daniels Midland. I received financial support from a U.S. Department of Education GAANN Fellowship and from a National Science Foundation Graduate STEM Fellowship in K-12 Education.